Energy Advances

ROYAL SOCIETY OF CHEMISTRY

REVIEW ARTICLE

View Article Online
View Journal | View Issue



Cite this: *Energy Adv.*, 2022, 1, 580

# A critical review of technologies, costs, and projects for production of carbon-neutral liquid e-fuels from hydrogen and captured $CO_2$

Harpreet Singh, * Chengxi Li, Peng Cheng, Xunjie Wang and Qing Liu

Hydrogen production along with CCUS (carbon capture, utilization, and storage) are two critical areas towards decarbonization and transition to net-zero from the current fossil fuel-based energy system. Although some technical challenges and relatively high costs of these technologies are the limiting factors for their wide-scale use in the short term, the other challenge in the mass-adoption of these technologies is the lack of the hydrogen- and $CO_2$-compatible midstream (transport, pipelines, storage, *etc.*) and downstream (engines, turbines, *etc.*) infrastructure, especially as it is related to the scale required for their wide adoption. The widespread infrastructure to support the large-scale hydrogen ($H_2$) economy with CCUS is not expected to be ready before 2030 in any part of the world, although the social and legal obligations to decarbonize energy and other infrastructure-heavy sectors are moving much faster. The lack of compatible midstream and downstream infrastructure is limiting the large-scale utilization of $H_2$, and captured $CO_2$ can be partially offset by producing sustainable liquid electro-fuels (e-fuels) derived from $H_2$ and captured $CO_2$. The carbon-neutral liquid e-fuels derived from $H_2$ and captured $CO_2$ are attractive for multiple reasons, which include (i) being compatible with existing infrastructure for storage and transportation, (ii) being compatible with existing internal combustion engines in aviation, shipping, freight, *etc.*, without requiring any modification to the engine or other equipment, (iii) being low in sulfur and being also able to be mixed with kerosene produced using fossil fuel, and (iv) huge transport market for their fossil fuel-based counterparts, with potential for greater long-term returns in view of their contribution in reducing carbon emissions from this sector. In terms of the technology readiness level and the field experience, liquid e-fuels have been produced at various pilot and industrial scales worldwide without any technical barriers. This study reviews a large number of technologies for $H_2$ production (16 technologies), $CO_2$ capture (7 technologies), their performance data, and the costs. Further, this study reviews the processes, including reactions, catalysts, and costs, to produce two liquid e-fuels (e-methanol and e-kerosene) that can be used as carbon-neutral alternatives to their fossil fuel-based conventional counterparts. The current and future projects for commercial production of liquid e-methanol and e-kerosene are also reviewed. Finally, the outlook and challenges to produce liquid e-fuels are discussed along with recommendations.

Received 7th July 2022,
Accepted 8th August 2022

DOI: 10.1039/d2ya00173j

rsc.li/energy-advances



## 1 Introduction

For reaching net-zero by 2050, global $H_2$ production needs to grow 80–95% per annum from the current $H_2$ production of ~120 MM tonnes per annum (tpa) according to the "Mission Possible" report.[1] As per the global carbon-neutral goal by 2050 and sustainable development scenario (SDS), carbon capture, utilization, and storage (CCUS) capacity worldwide must increase from 40 MM tpa in 2020 to 800 MM tpa by 2030.[2] According to the IEA[2,3] the net-zero emission goal is virtually impossible to achieve without CCUS. The countries in Asia Pacific, the world's most populous and fastest-growing region economically, emit about half of the global greenhouse gas (GHG) emissions. The energy demand in Asia Pacific over the next two decades is expected to be almost two-thirds of the global energy demand growth, and a large part of that demand will be likely met by hydrocarbons. Demand for some key fossil fuel-based hydrocarbons can be met by carbon-neutral liquid e-fuels produced using $H_2$ and captured $CO_2$ to a reasonable degree in the medium-term, whereas e-fuels will completely substitute fossil fuels in some key industries (*e.g.*, aviation) by 2050.

There is wide interest in $H_2$ as a fuel in the mobility (FCEVs, HICE), power generation (gas turbines or fuel cell power plants),

*CNPC USA, Houston, Texas 77042, USA. E-mail: harpreet.singh@cnpcusa.com*

and other industries (steel, chemical, heat, *etc.*) according to the routes listed in Fig. 1. Among these different options where $H_2$ can be integrated within the economy, the primary demand growth drivers of $H_2$ are expected to be transportation and industrial uses. In contrast, the use of hydrogen as a fuel for power generation (electric and gas utilities) is unlikely to be its growth driver because of high production costs and efficiency losses which make $H_2$ too expensive in power generation;[4] however, despite the cost disadvantage, the motivation for using $H_2$ in power generation at present is primarily to meet decarbonization

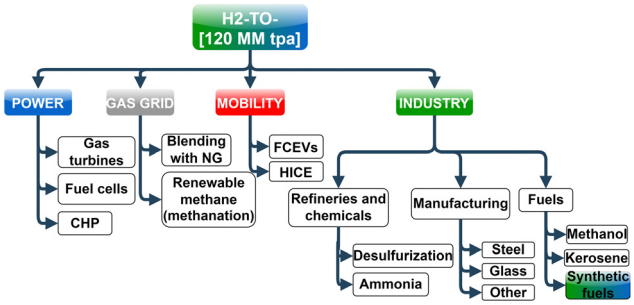


Fig. 1 A list of available routes to integrate hydrogen in various sectors of the economy, including power, gas, mobility, and industry.

**Harpreet Singh**

*Harpreet Singh is a Petroleum Engineer at CNPC USA, where he is leading the projects on New Energy (CCUS, Hydrogen) and Unconventional Oil and Gas Fracturing Technologies in North America. At CNPC USA, he is also actively contributing to projects on Digital Trends in Oil and Gas Industry, and Reservoir Management and Field Development. Harpreet has 7+ years of professional working experience in the oil and gas industry and research lab. He holds MS and PhD degrees in Petroleum Engineering from the University of Texas at Austin and a bachelor's degree from the Indian Institute of Technology, Roorkee.*

**Chengxi Li**

*Chengxi Li graduated from the Massachusetts Institute of Technology with a PhD in mechanical engineering. He researches technologies in new energy (e.g., CCUS), machine learning methods in drilling engineering, finite element analysis, and offshore wind technologies.*

**Peng Cheng**

*Dr Peng Cheng is the Vice President for CNPC USA, a global R&D center of China National Petroleum Corporation (CNPC). He has 20+ years of engineering experience and 15+ years of Oil & Gas experience mainly focused on completions and stimulations technology. Dr Cheng holds a PhD degree in mechanical engineering from Columbia University in the City of New York, a BS and an MS degree in mechanical engineering, both from Tsinghua University in China.*

**Xunjie Wang**

*Dr Xunjie Wang joined Beijing Huamei Inc., a subsidiary company of China National Petroleum Corporation (CNPC), in 2019. He has over 20 years of experience in petroleum engineering focused on Wireline Logging and Petroleum Geology. Dr Wang holds a PhD degree in Petroleum Engineering from the Research Institute of Petroleum Exploitation and Development, CNPC, China, and an MS degree in Sedimentology from China University of Petroleum.*

**Qing Liu**

*Dr Qing Liu is a Senior Engineer at CNPC USA, a global R&D center of China National Petroleum Corporation (CNPC). She holds a PhD degree in Control Theory and Control Engineering from China University of Petroleum, and an MS degree in automation engineering from Tianjin University in China. Dr Liu has 6+ years of electrical engineering experience and 10+ years of Oil & Gas experience mainly focused on Control Technology.*

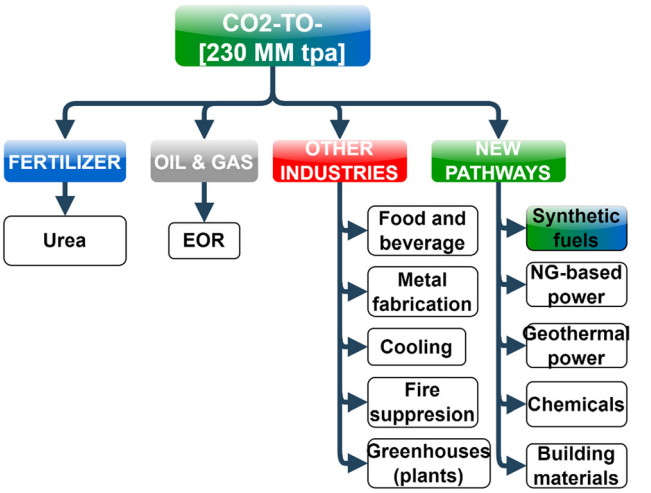


Fig. 2 Utilization of $CO_2$ as a valuable commodity in various sectors of the economy, including new pathways, such as fuels and chemicals.

goals, increasing interest in renewable energy and energy storage. The growing potential of hydrogen in the power sector will require lower costs, refurbishing existing coal and gas power plants that enable burning $H_2$-rich fuels, and creation of markets and hubs. Similarly, global consumption of $CO_2$ in 2019 was estimated to be 230 MM tpa[5] (with ~57% in urea and 34% in EOR) for applications shown in Fig. 2, and it is expected to grow to 272 MM tpa by 2025. Unlike $H_2$, the price of $CO_2$ varies significantly based on the region and the industry, such that the price of $CO_2$ can range from \$3 to >\$400 per ton and its supply is closely related to ammonia and fertilizer manufacturing.[5]

Although $H_2$ can be integrated into various sectors of the economy through power, gas, mobility, and industry based on the routes listed in Fig. 1, it needs $H_2$-compatible midstream and downstream infrastructure that remains uncertain to predict in terms of its development and timeline. The diverse applications of $H_2$ would require the deployment of large-scale infrastructure, but despite the potential economic and environmental prospects from these applications, securing investment for midstream and downstream infrastructure that typically involves a wide number of stakeholders is challenging due to the lack of a clear business model.

With the challenge mentioned above in securing investment for $H_2$-compatible infrastructure, the most realistic application for large-scale utilization of $H_2$ in the near- to mid-term is to produce liquid electro-fuels (e-fuels) derived from $H_2$ and captured $CO_2$ (*e.g.*, carbon-neutral synthetic methanol and kerosene) because of the following unique advantages of liquid e-fuels:

- Compatible with existing infrastructure for storage and transportation of liquid fossil fuels.
- Compatible with existing internal combustion engines (ICE) in aviation, shipping, freight, *etc.*, without requiring any modification to the engine or other equipment.
- Synthetic kerosene is low in sulfur and can also be mixed with conventional kerosene produced using fossil fuel.
- Having an existing market with huge demand and carbon-neutral liquid e-fuels are the only realistic options in the near- to mid-term in reducing carbon emissions at scale from road, maritime, and aviation transport.

Carbon-neutral e-methanol and e-kerosene are the two most important fuels that can be produced using captured $CO_2$ and $H_2$. More than 95 billion liters of methanol (~98 MM tpa) is manufactured every year, making it the world's most commonly shipped chemical commodity.[6] Methanol is a highly versatile chemical that is widely used in various applications, for instance, as a transportation fuel and as a feedstock to produce various chemicals/products. Further, the need for a high-energy-density liquid fuel in aviation is provided by kerosene, and its combustion is responsible for ~98% of emission in the aviation sector. The aviation sector is difficult to decarbonize because of its need for high energy-density liquid fuels like kerosene, which cannot be easily replaced in the coming decades. Currently, long-haul operational aircraft engines cannot operate on electricity or $H_2$; therefore, the concept of sustainable aviation fuel (SAF) is the only option to decarbonize aviation, which is enabled by a low-carbon kerosene (e-kerosene) produced using $H_2$ and captured $CO_2$. It is estimated[7] that 65% of carbon mitigation to achieve net-zero in the aviation sector by 2050 will be contributed by SAF. For this reason, SAF annual production is expected to increase[7] from the current 125 million liters to 5 billion by 2025 and potentially 30 billion liters by 2030. In the U.S., SAF production is expected to reach at least 3 billion gallons per year by 2030 which will reduce the emissions in aviation by 20%. For net-zero in aviation by 2050, the share of SAFs in jet fuel demand is expected to grow from 0% in 2019 to ~15% by 2030, 60–65% by 2040, and 100% by 2050.

The rest of the paper is organized as follows: Section 2.1 discusses the pathway to produce liquid e-fuels using $H_2$ and captured $CO_2$, including the status of $H_2$ production and $CO_2$ capture technologies. Sections 2.2 and 2.3 review the technologies to produce $H_2$ and capture $CO_2$, including their performance data and costs. Section 2.4 reviews the technologies required to produce e-methanol and SAF, including the processes, reactions, catalysts, and costs. Sections 3.1 and 3.2 review the current and future projects for commercial production of e-methanol and SAF. The final section discusses the outlook and challenges in producing liquid e-fuels along with recommendations.

## 2 Method and technologies

### 2.1 Pathways and summary of technology readiness

Although $H_2$ can be used as a fuel directly, the infrastructure required to support large-scale application of $H_2$ does not yet exist. Therefore, liquid electro-fuels (e-fuels) derived from $H_2$ and captured $CO_2$ are attractive for multiple reasons, which include (i) being easier to store than gaseous or liquid $H_2$, (ii) being able to be transported using existing petroleum infrastructure, and (iv) being compatible in aviation, shipping, freight, *etc.*, without any modification to engines or equipment.

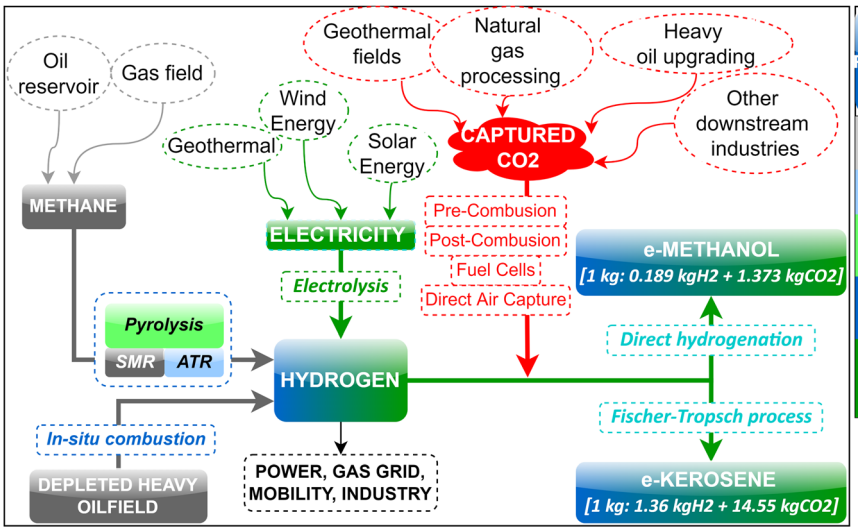


| HYDROGEN PRODUCTION METHOD | TRL (1-9) | COST [$/kg H2] w/o CCS | COST [$/kg H2] with CCS |
|---|---|---|---|
| SMR | 9 | 2.08 | 2.27 |
| ATR | 7-9 | N/A | 1.48 |
| Pyrolysis | 3-5 | 1.59-1.70 | |
| In-situ combustion | 3-5 | < 2 | |
| Electrolysis (PEM or Alkaline) | 6-9 | > 2 (Variable) | |

*e-Methanol Cost [$/kg]: ~[0.16, 1.26]*
*e-Kerosene Cost [$/gal]: ~[4.30, 6.78]*

Fig. 3 A schematic illustrating the use of oil and gas resources to produce carbon-neutral liquid e-fuels. Hydrogen can be processed with captured $CO_2$ to produce carbon-neutral liquid e-fuels (*e.g.*, e-methanol, e-kerosene) which (i) are compatible with existing engines, (ii) are easier to store, and (iii) can be transported using existing petroleum infrastructure.

Fig. 3 shows a summarized overview of strategies to integrate $H_2$ production and low-carbon e-fuels derived from $H_2$ through existing oil and gas resources and infrastructure. Specifically, $H_2$ can be produced either from fossil fuels directly or through electrolysis that runs on electricity provided by geothermal reservoirs. Hydrogen can either be used directly for its various applications listed in Fig. 1, or further processed with captured $CO_2$ and converted to e-methanol and/or e-kerosene.

A summary of all major and novel state-of-the-art $H_2$ production and $CO_2$ capture technologies in terms of the technology readiness level (TRL) (minimum of 1 indicating the basic principles observed and maximum of 9 indicating the actual system proven in the operational environment) is presented in Table 1. The technologies listed in Table 1 for $H_2$ production and $CO_2$ capture are discussed in detail in the following sections, including their performance data and costs.

## 2.2 Hydrogen production

**2.2.1 Comparison of technologies.** Hydrogen production technologies that are expected to play an important role in producing large-scale $H_2$ in short- to long-term, along with their advantages, disadvantages, TRL, and range of cost, are presented in Table 2. The production of $H_2$ is categorized into 4 categories, which are $H_2$ produced from fossil fuel, from biomass and waste-stream, from electrolysis of water, and from natural free-state occurrence. Hydrogen can be produced from fossil fuels using seven methods,[8–16,18,19] which are coal gasification, steam reforming (or popularly known as steam methane reforming when methane is used as a feedstock), plasma reforming, partial oxidation (POX), auto-thermal reforming (ATR), pyrolysis of methane, and *in situ* combustion of underground reservoirs. Hydrogen can also be produced from biomass and waste-stream[20,21] using the three technologies discussed here, which are dark fermentation, photofermentation, and gasification. The third category of $H_2$ production is by electrolysis of water,[8–13,30,31] which refers to splitting water into $H_2$ and oxygen molecules using electricity, and within this category three technologies are discussed, which are alkaline electrolyzers, solid oxide electrolyzers, and polymer electrolyte membranes (PEM), respectively. Finally, the last category of $H_2$ production through its natural occurrence in geological media[22–29] is considered to be the least known, but it offers the potential to produce large-scale $H_2$ most economically among all methods.

*2.2.2.1 SMR with membrane reactors.* Although $H_2$ production through SMR is mostly through conventional reactors, membrane reactors have the potential to improve energy efficiency and conversion efficiency, and reduce costs (relaxed operating conditions) through process intensification measures like (i) membrane reactors that combine multiple processes into a single unit (*e.g.*, reaction and purification) and (ii) low-carbon sources of heat and energy (*e.g.*, microwave heating, plasma, *etc.*). The SMR performance data with different membrane reactors and their operating conditions is presented in Table 3.

*2.2.2.2 Electrolysis*

*2.2.2.2.1 Electricity consumption.* Solid oxide electrolyzers are technically less mature, but they offer the highest efficiency among all types by combining heat and electricity to produce $H_2$. The comparison of three main technologies for electrolysis of water in terms of their performance as a function of current–voltage (electricity consumption) data is presented in Fig. 4, which shows that solid oxide electrolyzers consume the least amount of electricity, while alkaline electrolyzers consume the most electricity.

*2.2.2.2.2 Startup time.* Of these three different types of electrolyzers, alkaline electrolyzers are technically the most

Table 1 Status of $H_2$ production and $CO_2$ capture technologies[8–39] in terms of their technology readiness level (TRL)

| TRL (# and description) | | $H_2$ production technologies | $CO_2$ capture technologies |
|---|---|---|---|
| 1 | Basic principles observed | • Natural free-state geological occurrence | |
| 2 | Technology concept formulated | | |
| 3 | Experimental proof-of-concept | • Photoelectrochemical water-splitting | • Post-combustion ionic liquids<br>• BECCS power<br>• Pre-combustion low-T separation<br>• Dense inorganic membranes<br>• Hydrate-based capture |
| 4 | Technology validated in lab | •Thermochemical water-splitting | |
| 5 | Technology validated in the industrial environment | • Pyrolysis of methane<br>• *In situ* combustion of hydrocarbon reservoirs<br>• Dark fermentation of biomass<br>• Photofermentation of biomass<br>• Solid-oxide electrolysis water-splitting | • Dense inorganic membranes ($H_2$ separation for reformer) |
| 6 | Technology demonstrated in the industrial environment | • Plasma reforming<br>• Gasification of biomass | • Polymeric membranes (power plants and NG processing)<br>• Post-combustion biphasic solvents<br>• CLC<br>• CaL |
| 7 | System prototype demonstrated in the operational environment | | • Polymeric membranes (NG industry)<br>• Pre-combustion IGCC + CCS<br>• Oxy-combustion coal power plant<br>• Post-combustion adsorption<br>• BECCS industry<br>• DAC (adsorbents and absorbents)<br>• Cryogenic (solid $CO_2$)<br>• Fuel cell capture |
| 8 | System complete and qualified | • Proton exchange membrane electrolysis water-splitting | • Oxy-combustion gas turbine<br>• Pre-combustion PSA with cryogenic (liquid $CO_2$) |
| 9 | Actual system proven in the operational environment | • Coal gasification<br>• Steam reforming<br>• Partial oxidation<br>• Auto-thermal reforming<br>• Alkaline electrolysis water-splitting | • Post-combustion amines (power plants)<br>• Pre-combustion NG processing (gas sweetening) |

BECCS: bioenergy with carbon capture and storage. NG: natural gas. CLC: chemical looping capture. CaL: calcium carbonate looping. IGCC: integrated coal gasification combined cycle. PSA: pressure swing adsorption. DAC: direct air capture.

mature, but they have several limitations when working with intermittent renewable energy sources. PEM electrolyzers overcome some of the limitations of alkaline electrolyzers, including (i) integration with fluctuating renewable energy power systems and (ii) a faster response time, as shown in Fig. 5.[50] Most commercially-available PEM electrolyzers have input power limits of 5 MW and 10 MW as single units (also called stacks; a module is a combination of several stacks; a system is a combination of multiple modules), but these stacks can be grouped to form a bigger unit with a higher power limit.

*2.2.2.2.3 Efficiency versus system size.* According to the survey of commercially-available alkaline (from Pure Energy, McPhy, Hydrogenics, and IHT) and PEM (from Nel, ITM, Hydrogenics, and Areva) electrolyzers for a range of system sizes (0.1 kW to 100 MW),[51] it was found that gains in efficiency with the increase in system size reaches a plateau around 100–300 kW size for both types (alkaline and PEM) of electrolyzers, as shown in Fig. 6; the reason for the plateau in efficiency is likely due to modular stacks above a certain scale.[51] The highest efficiency (or lowest power consumption) for alkaline and PEM electrolyzers is $\sim$50 kW h $kg^{-1}$ and $\sim$55 kW h $kg^{-1}$, respectively.

### 2.3 $CO_2$ capture

**2.3.1 Comparison of technologies.** There are 7 major carbon capture technologies, which are listed in Table 4. The two most popular capture technologies are post-combustion and gas sweetening, primarily due to a large number of industrial applications in which $CO_2$ is separated using these two technologies; power plants use post-combustion to capture $CO_2$ from the flue gas through regenerative solvents, while natural gas processing facilities capture $CO_2$ through the gas sweetening process.

**2.3.2 Technology performance data.** Table 5 shows the empirical data[66,67] reported by the EDGAR (Energy Delta Gas Research) $CO_2$ purity project, which present the levels of impurities in captured $CO_2$ stream from different capture technologies. Table 5 demonstrates that post-combustion (amine solvent-based $CO_2$ absorption) provides the highest level of purity in captured $CO_2$, but with a large variation in the levels of impurities.

The minimum energy required (as estimated from the combined first and second laws of thermodynamics) to capture $CO_2$ (with a known starting $CO_2$ concentration) increases sharply with a slope of $\sim -11$ kJ $mol_{CO_2}^{-1}$ for $CO_2$ concentration lying between 0.4 and 0.05, and with a slope of $\sim -220$ kJ $mol_{CO_2}^{-1}$ for $CO_2$ concentration below 0.05 in the

gas mixture.[68] Specifically, capturing $CO_2$ from the most concentrated source, such as fuel gas from coal gasification, flue gas from coal and natural gas oxidation, *etc.*, requires relatively less energy between 1 and 4 kJ $mol_{CO_2}^{-1}$, compared to capturing $CO_2$ from air using DAC (with ~0.04% or 409 ppm $CO_2$ concentration), which requires between 19 and 21 kJ $mol_{CO_2}^{-1}$.

Table 2 Summary of technologies for production of hydrogen[8–38] at a medium to large scale. Each technology is color-coded to depict the greenhouse gas emissions associated with the produced $H_2$, where grayish blue represents the technology with the largest amount of emissions and dark green represents the technologies with the least amount of emissions2.2.2 Technology performance data

| Class | Technology | Description | Advantages | Disadvantages | TRL (max. 9) | Cost [$ per kg $H_2$] |
|---|---|---|---|---|---|---|
| From fossil fuels | Coal gasification | Steam and oxygen are used for combustion and reacted with coal | Simpler emission control over conventional combustion | Produces $CO_2$ and other pollutants | 9 (6–7 with CCS) | 1.34 (without CCS)–1.63 (with CCS) |
| | Steam reforming (SR) | The steam created by combustion with air is reacted with the feedstock and catalyst. Endothermic | Mature technology and easier to scale up | Produces $CO_2$ | 9 (7–8 with CCS) | 2.08 (without CCS)–2.27 (with CCS) |
| | Plasma reforming | Similar to SR, but uses high temperature electric heat from plasma devices instead of steam | Does not require a catalyst. Reduced reactor size and weight | High electricity requirements. Produces $CO_2$ | 5–6 | <2.08 |
| | Partial oxidation (POX) | Steam created by combustion with partial use of oxygen. No catalyst used. Exothermic | Faster start-up times and relative compactness. No catalyst required | Produces $CO_2$ | 9 | 1.48 (with CCS) |
| | Auto-thermal reforming (ATR) | Combination of steam reforming and partial oxidation | Faster response times. Simpler and cheaper than SR. Compact design relative to other fossil fuel-based methods | Produces $CO_2$. Requires pure oxygen or air separation unit. Limited commercial experience | 9 (7–8 with CCS) | 1.48 (with CCS) |
| | Pyrolysis of methane | Uses a catalyst to crack methane at high temperature in the absence of oxygen | No $CO_2$ emission. Produces solid carbon | Co-produces tar that can plug the reactor | 3–5 | 1.59–1.70 |
| | *In situ* combustion of hydrocarbon reservoirs | Steam/air/oxygen injection in fossil fuel-bearing reservoirs | Unwanted gases are not produced via downhole purification. Low-cost production | Complex *in situ* combustion that is difficult to control and predict | 3–5 | <2 |
| From biomass and waste-stream | Dark fermentation | Wet biomass. Uses anaerobic bacteria under dark conditions | Relatively simple technology. Waste recycling. $CO_2$-neutral process. | Low yield of $H_2$ relative to reactor volume. | 4–5 (3–5 with CCS) | 2.57 |
| | Photo fermentation | Wet biomass. Uses anaerobic bacteria and light | Relatively simple technology. Waste recycling. $CO_2$-neutral process | Low yield of $H_2$ relative to reactor volume | 4–5 (3–5 with CCS) | 2.83 |
| | Gasification | Dry biomass. Uses a controlled amount of oxygen and/or steam. No bacteria required. | Relatively simple technology. Waste recycling. $CO_2$-neutral process. | Pre-treatment cost. Fluctuating $H_2$ yields because of feedstock impurities. Co-produces tar | 5–6 (3–5 with CCS) | 1.77–2.05 |

| Class | Technology | | Description | Advantages | Disadvantages | TRL (max. 9) | Cost [$ per kg $H_2$] |
|---|---|---|---|---|---|---|---|
| From water-splitting | Thermochemical process | | Produces $H_2$ by splitting water through a series of high-temperature (800–900 °C) chemical reactions by using heat as the input energy. A single step conversion of water to $H_2$ through direct thermolysis is possible, but not practical as it requires extremely high temperature (>2500 °C) | Suitable for large-scale production capacity that is larger than the scale of $H_2$ refueling station. Can utilize sunlight and/or heat from nuclear waste | Requires additional $H_2$ distribution network due to its large-scale production capacity. Commercial viability is currently challenging | 2–4 | 3.70 |
| | Photoelectrochemical (PEC) process | | Produces $H_2$ by splitting water through semiconductor immersed in a water-based electrolyte that uses visible light as the input energy | Low operating temperatures and cost-effective materials (thin-film, particle semiconductor). Can utilize an unlimited source of solar light | Very low solar-to-$H_2$ conversion efficiency (< 3%). Low current density due to reduced area of electrolysis in solar cell | 2–3 | 5.70 |
| | Electrolysis | Alkaline | Electrolysis process converts water directly into $H_2$ and oxygen (without any partial reactions with other chemicals/compounds) by using electricity as an input energy. Primary electrolysis components consist of an anode and a cathode separated by an electrolyte. | Mature technology. The first water splitting technology to be developed. Relatively low cost | Corrosive liquid electrolyte. Perform poorly with fluctuating power sources, because of a slow response (startup) time. | 9 | 2.30 (with $0.037 per kW h as the electricity cost) |
| | | Solid-oxide | | Can leverage both heat and electrical energy | Require high temperature (>700-800 °C). Slower start-up time | 5 | 2.30 (with $0.037 per kW h as electricity cost) |
| | | Polymer electrolyte [or proton exchange] membrane (PEM) | | Can operate at high current densities. Perform better with fluctuating input currents. Integrate better with variable power generation, such as wind and solar. Faster response time | Expensive materials that add to the cost. Scale-up to the MW scale is a challenge. | 6–8 | 2.30 (with $0.037 per kW h as electricity cost) |
| Natural free-state occurrence | | | Naturally occurring free-state $H_2$ found in geological media. | Can be extracted using existing oil and gas drilling technology. | Its geology of occurrence is not well-understood. | 1 | Most economical |

**2.3.3 Cost of capture.** The CCUS technology is about ~15 years old. However, the costs related to capture technology, which can be up to 40% of the entire project, can vary significantly due to the nature of the capture technology that is still evolving. The cost of capture varies by industry, from $15 per ton to $342 per ton, depending on the concentration of the emitted $CO_2$ in the flue stream[69] as shown in Fig. 7, which indicates that a higher concentration of $CO_2$ (red colored legend) leads to a lower capture cost. Most of the $CO_2$ emissions in the oil and gas industry are highly concentrated, such as in natural gas processing, chemicals, and $H_2$ production by steam methane reforming.

The capture costs are the largest in the CCUS value chain, followed by the costs for compression and dehydration of $CO_2$, and then the cost of transporting $CO_2$, typically by pipelines.[70] The lowest costs in the CCUS are for the injection and MMV of stored $CO_2$, which is typically less than 10% of the total cost.

**2.3.4 Capture technologies adopted by the oil and gas companies.** Few oil and gas companies have chosen the capture technologies either for their own operations or as a service,

Table 3 SMR performance data with membrane reactors

| Membrane ↓ | Thickness (μm) | Area ($cm^2$) | $T$ (K) | $\Delta P$ (kPa) | $H_2$ permeance (mol $m^2$ $S^{-1}$ $Pa^{-0.5}$) | $H_2/N_2$ selectivity | Catalyst | GHSV ($h^{-1}$) | S/C ratio | Sweep (mol $h^{-1}$) | $CH_4$ conversion (%) | Source |
|---|---|---|---|---|---|---|---|---|---|---|---|---|
| Pd–Ru/PSS | 100 | 1.2 | 773 | 100 | $1.10 \times 10^{-4}$ | ND | Ni | 30 | 3 | 0.4 | 80 | 40 |
| Pd/PSS | 11 | 20 | 800 | 100 | $1.10 \times 10^{-3}$ | ND | Ni | 1120 | 3 | 1.3 | 82 | 41 |
| Pd/$A_{l2}O_3$ | 3.8 | 155 | 823 | 2500 | $3.70 \times 10^{-3}$ | 97 | Ni | 150 | 3 | 0.13 | 91 | 42 |
| Pd-Alloy/PCS[a] | 7.3 | 93.3 | 823 | 800 | $2.20 \times 10^{-3}$ | ND | Ni | 3000 | 3 | None | 68 | 43 |
| Pd | 11 | 35.8 | 873 | 1600 | $1.70 \times 10^{-3}$ | 3000 | Ni | 600 | 3 | None | 37 | 44 |
| Pd–Ru/PSS[b] | 5 | 13.3 | 853 | 2900 | $2.70 \times 10^{-3}$ | 200 | Ni | 150 | 3 | None | 85 | 45 |
| Pd–Au/PSS | 5 | 16.1 | 784 | 2800 | $2.40 \times 10^{-3}$ | 6400 | Ru | 147 | 3 | None | 94 | 46 |
| Pd-Based | 13 | 44 | 673 | 300 | $3.80 \times 10^{-3}$ | 9000 | Ni | 2600 | 3.5 | 1.36 | 84 | 47 |
| Pd–Ru/PSS | 6 | 100 | 773 | 253 | $3.50 \times 10^{-3}$ | 59 | Ni | 837 | 3 | None | 77.5 | 48 |
| Pd-Based/PSS | 4–5 | 175 | 823 | 1013 | $2.40 \times 10^{-3}$ | 618 | Ru | 2000 | 3 | None | 82 | 49 |

ND: no data. GHSV: gas hourly space velocity. S/C: steam-to-carbon. [a] Porous ceramic support. [b] Porous stainless-steel support.

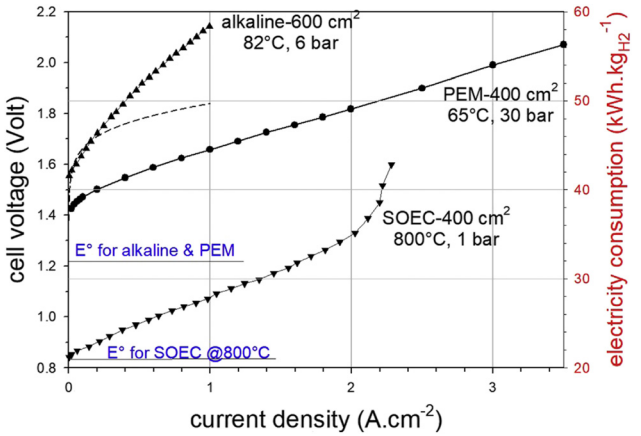


Fig. 4 Comparison of alkaline, PEM, and solid oxide electrolyzer cell (SOEC) technologies for electrolysis of water as a function of electricity consumption (current and voltage).[31] The indicative temperatures and pressures for each technology are a general representative of their operating conditions.

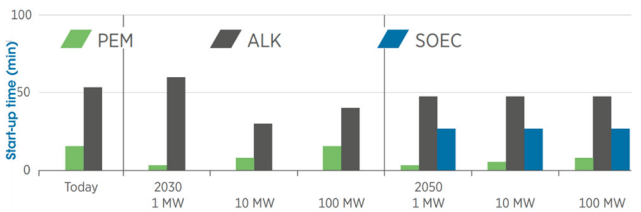


Fig. 5 Comparison of start-up times for PEM, alkaline (ALK), and solid oxide electrolyzer cell (SOEC) technologies.[50]

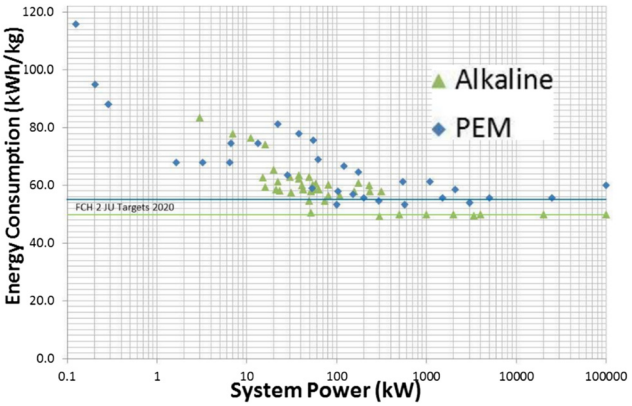


Fig. 6 Electrolysis energy consumption (indicator of efficiency) *versus* system size of the alkaline (from Pure Energy, McPhy, Hydrogenics, and IHT) and PEM (from Nel, ITM, Hydrogenics, and Areva) electrolyzers for a range of commercially available electrolyzers.[51]

where some of the notable companies are Oxy, Shell, Baker Hughes, and ExxonMobil.

Oxy is deploying the world's largest direct air capture (DAC) facility in the Permian Basin (referred to as DAC-1) to use captured $CO_2$ for enhanced oil recovery (EOR), which is currently in the front-end engineering and design phase and expected to be online by early 2024.[71] The DAC-1 facility will extract up to 1 MM tpa of $CO_2$ (at a cost of ~$500 MM) with >99% purity from air, which is equivalent to the annual emissions of about 215 000 cars. Additionally, Oxy is planning to build 70 DAC facilities by 2035, each with up to 1 MM tpa capture capacity, where the oil produced using this captured $CO_2$ through EOR will be marketed as net-zero oil. Oxy signed its first contract to supply 200 000 bbl per year of net-zero oil (produced using $CO_2$ captured from DAC facilities) for 5 years to SK Trading International, based in Seoul, South Korea.[72]

Shell has been testing various capture technologies in collaboration with other partners in Europe, and it has now decided to use solid sorbents in place of liquid solvents while moving from demonstration-scale to large-scale operations. Shell plans to scale solid adsorbent technology from current 1 tpd to 150 tpd by 2024 with an eventual target of 1000–2000 tpd commercial plants.[73] Shell's solid adsorbent technology can separate over 90% of the $CO_2$ from post-combustion flue gases with 95% purity, and it is reported to be 40% cheaper than liquid amine technology.

Baker Hughes has three carbon capture technologies,[74] which are (i) chilled ammonia process (CAP), (ii) mixed salt process (MSP), and (iii) compact carbon capture (CCC). Of these three technologies, CAP is a post-combustion technology (with a TRL of 7) based on a non-proprietary solvent formulation that uses readily available ammonia to capture $CO_2$ from low-pressure flue gases generated by point-sources of emissions, such as fossil-fuel-based power plants, waste-to-energy

Table 4 Carbon capture technologies, the output, major industrial applications, and the $CO_2$ capturing medium[39,52–65]

| Characteristics ↓ | Pre-combustion | Post-combustion | | | | | |
|---|---|---|---|---|---|---|---|
| | | Traditional method | Specialized methods | | | | |
| | | | Cryogenic | Oxyfuel combustion | Chemical looping | Fuel cells | DAC |
| Source of $CO_2$ emission | Syngas coming from gasification units prior to combustion | Flue gas due to combustion with air and fuel | Flue gas due to combustion with air and fuel | Flue gas due to combustion with oxygen and fuel. $O_2$ is supplied externally from an air separation unit | Flue gas due to combustion with oxygen and fuel. $O_2$ is extracted internally from the solid-state oxygen carrier through reduction–oxidation reactions | Flue gas due to combustion with air (and/or oxygen) and fuel | Air. No combustion |
| Capture mechanism | Sorption with pressure and/or temperature swing | Sorption with pressure and/or temperature swing | Direct phase change from gas to liquid/solid | Sorption with pressure and/or temperature swing | Sorption with pressure and/or temperature swing | FCs pump $CO_2$ through the electrolyte to separate $CO_2$ *via* selective ionic transport | Membrane separation and/or sorption |
| $CO_2$ capturing agents | Solvents and membranes | Solvents, membranes, and adsorbents | Cryogenic cooling with liquid solvents | Solvents and membranes | Solvents and membranes | Electrochemical system | Adsorbents and membranes |
| Outputs | $CO_2$ and $H_2$ | $CO_2$ and $N_2$ | $CO_2$, $N_2$, SOx, NOx, and Hg | $CO_2$ and steam | $CO_2$ and $O_2$ | $CO_2$, water, and some $H_2$ | $CO_2$ and air |
| Advantages | High capture efficiency | Most mature technology | A high concentration of $CO_2$ is captured | Leads to a high concentration of $CO_2$ in flue stream, which is easier to capture | Cost-effective option to oxy-combustion, but with similar benefits | Very high capture efficiency. Cheaper. Can also utilize $CO_2$ as the working fluid | Can capture $CO_2$ anywhere on the earth without the need for point-source emission |
| Disadvantages | Less mature technology | Lower capture efficiency | Relatively high CAPEX | Relatively high CAPEX | Less mature technology | Less mature technology | Relatively high CAPEX |
| Major industrial sectors | Power and industrial gases | Power and cement | Power and cement | Power and steel | Power and steel | Power and industrial gases | Greenhouse and carbonated beverages |

Table 5 Carbon capture technologies and the corresponding level of impurities in the captured $CO_2$ stream. Adapted and expanded after ref. 66 and 67

| | Pre-combustion | | | | Post-combustion | DAC | | | Oxyfuel combustion |
|---|---|---|---|---|---|---|---|---|---|
| Capture technologies → | Selexol IGCC | Reactisol IGCC | Amine scrubbing | Sour SEWGS | Amine scrubbing | Adsorption | Absorption | Membrane | Oxyfuel and double flashing |
| $CO_2$ | 98.1–99.7% | 95–98.5% | >97.2% | >99% | 99.8–99.9% | 30–90% | 90–99% | 2.5–20% | 97% |
| $H_2$ | 1.50% | 20 ppm | <1% | <1% | — | — | — | — | — |
| $O_2$ | — | — | — | — | 150–300 ppm | — | — | — | 1.20% |
| $N_2$ | 195 ppm | <1% | <1% | <1% | 450–900 ppm (inc. Ar) | — | — | — | 1.60% |
| Ar | 178 ppm | 150 ppm | <1% | <1% | 450–900 ppm (inc. $N_2$) | — | — | — | 0.40% |
| Sulfur compounds | $2 < H_2S <$ 1700 ppm | 0.2–20 ppm | $H_2S$ < 200 ppm for the 2-stage plant | <5000 ppm to ppm level with $H_2S$ stage | 10–20 ppm ($SO_2$ predominantly) | — | — | — | 35 ppm $SO_2$ |
| NOx | — | — | — | — | 20–40 ppm | — | — | — | 150 ppm |
| CO | 100–1300 ppm | 400 ppm | <1% | <1% | 10–20 ppm | — | — | — | — |
| $CH_4$ | 112 ppm | 100 ppm | <1% | <1% | — | — | — | — | — |
| MeOH | — | 20–200 ppm | — | — | — | — | — | — | — |
| $H_2O$ | 376 ppm | 0.1–10 ppm | 1.80% | 500 ppm (drying step) | 100–600 ppm | — | — | — | — |




Fig. 7 Range of $CO_2$ concentration in % (red colored legend) and the corresponding carbon capture costs in $ per ton of $CO_2$ captured (blue colored legend) for specific industrial applications. The figure was created using the data from ref. 5.

power plants, biomass power plants, cement plants, refineries, and petrochemical complexes. The MSP capture technology (acquired from SRI International) is a post-combustion technology that uses a non-amine solvent (widely available and environmentally friendly) formulation based on commodity chemicals with reduced energy consumption and greater efficiency in the form of negligible solvent-degradation and reduced water use. Baker Hughes' CCC technology (acquired from 3C) uses solvent-based rotating packed beds. Solved-based rotating packed beds are compact (75% smaller and 50% cheaper than conventional amine capture), modular (easy installation and retrofittable), and solvent-agnostic. The capture capacity of Baker Hughes' CCC technology is 250–500 tpd of $CO_2$ with >99% purity.

ExxonMobil has invested in Global Thermostat (a U.S.-based DAC company founded in 2010) and using its technology to deploy DAC at Haru Oni Project (Punta Arenas, Chile), which is an e-methanol (renewable methanol) plant anticipated to be completed by mid-2022.[75]

### 2.4 Liquid e-fuel production

Catalytic $CO_2$ reduction to produce high-value fuels is a major pursuit towards sustainable production of carbon-neutral fuels to reduce atmospheric carbon emissions. The low-carbon fuels possible to be produced by reacting $CO_2$ with $H_2$ can range from as simple as methane, ethane (precursor to ethylene, which is used to make plastics), and propane (for heating and cooking), to other commercially high-value liquid e-fuels that include methanol and SAF (synthetic jet fuel).

Conversion of $CO_2$ to liquid e-fuels can be through either a one-step or a two-step process, depending on the efficacy of the catalyst, which is a key ingredient in the process that seeks to activate chemical reactions without being consumed itself in the process. A one-step process converts $CO_2$ directly to liquid fuels, whereas the two-step process converts $CO_2/H_2$ to $CO/H_2O$ in the first reaction (called reverse water gas shift), followed by the second reaction that combines CO with $H_2$ to form the liquid fuel. The majority of catalysts that enable conversion of $CO_2$ to liquid fuels have limitations in terms of either the efficiency of conversion to liquids (selectivity) and/or the rate of formation of liquids. Besides the reactor design that can facilitate optimum operating conditions for the reactions, appropriate catalyst selection is key to the performance of the process to convert $CO_2/H_2$ to high-value liquid e-fuels. The technologies involved in producing e-methanol and SAF, including the process, reactions, and catalysts, are discussed in the following sections.

### 2.4.1 e-Methanol production

*2.4.1.1 Process.* Although almost all the methanol is conventionally produced *via* syngas where the CO and $H_2$ in the syngas react in an exothermic reaction to form methanol, methanol can also be produced renewably by direct hydrogenation of the captured $CO_2$ (Fig. 8) according to eqn (1) (direct hydrogenation) and (2) (reverse water gas shift).[76] The two reactants ($H_2$ and $CO_2$) are pressurized/compressed ($\sim$25 bar) before feeding them into the first reactor which operates at high temperature and high pressure[77] in case the initial pressures of the supplied $CO_2$ and $H_2$ are lower than the operating pressure of the synthesis reactor. The unused reactants following the methanol production, which are separated at the exit stream through condensation, can be recycled *via* a compressor and fed back into the reactor in addition to the fresh reactants. The formation of methanol is an exothermic process that generates heat, which is supplied for the endothermic reaction in the first reactor (Fig. 9).

One key operational difference between the traditional and sustainable methanol production is the significant production of water in the exit stream in the case of sustainable methanol production (approximately 30–40% water by mass in crude methanol), which reduces the activity and lifetime of the catalyst.[77]

Some of the key factors that influence the methanol synthesis are as follows:

- The composition of the syngas feed (when the produced $H_2$ is not pure).
- The converter designs to remove the heat of the exothermic reaction, which includes gas-cooled and steam-raising variants (axial, radial, and axial–radial configurations).

The three commercially used designs of the methanol synthesis reactor in the market are based on different heat transfer mechanisms, which include[79] (i) quench converter (direct cool *via* feed gas injection), (ii) tube-cooled converter (counter-current gas exchange), and (iii) steam-raising converter (isothermal bed temperatures). Of these three reactor designs, the tube-cooled converter (TCC) design enables the largest methanol production and carbon efficiency (moles of methanol in crude methanol to moles of CO and $CO_2$ in syngas) per unit volume of the reactor, whereas the quench-type reactor system typically contains the largest catalyst volume.[79]

*2.4.1.1.1 $H_2$ and $CO_2$ utilization.* Producing a kg of methanol requires 0.189 kg $H_2$ and 1.373 kg $CO_2$[80,81] under a limited conversion rate, or more specifically, according to the process flow diagram in Fig. 9, producing a kg of methanol requires an estimated 0.20 kg $H_2$ and 1.66 kg $CO_2$[78] with $BaCe_{0.2}Zr_{0.6}Y_{0.16}Zn_{0.04}O_3$ and Cu/Zn/Al as the catalysts for the RWGS reaction and the methanol synthesis, respectively. Few other studies[82–84] mention the net $CO_2$ utilization for e-methanol synthesis as 1.4t $CO_2$ per 1t of e-methanol (or equivalently, a kg of methanol requires 1.4 kg of $CO_2$), which is close to the other two numbers (1.373 kg $CO_2$[80,81] and 1.66 kg $CO_2$[78]).

*2.4.1.2 Reactions.* The synthesis of methanol through direct hydrogenation of $CO_2$ (eqn (1)) is an exothermic reaction, but it competes with the reverse water gas shift (RWGS) reaction, which is an endothermic reaction.[85] The synthesis of methanol requires retaining an equilibrium, such that at high temperatures the yield of methanol begins to decrease[77] as shown in Fig. 10, which means that an increase in temperature facilitates $CO_2$ activation to undesirable CO and $H_2O$, and reduces its equilibrium conversion rate.

Conversion of $CO_2$ to e-methanol can be either a one-step or a two-step process, where a one-step process converts $CO_2$ directly to liquid fuels, whereas the two-step process converts $CO_2/H_2$ to $CO/H_2O$ in the first reaction (*via* RWGS), followed by the second reaction that combines CO with $H_2$ to form e-methanol.

One-step process (direct $CO_2$ hydrogenation):

$$\underbrace{CO_2}_{\text{captured}} + 3\ \underbrace{H_2}_{\text{green or blue}} \overset{\text{catalyst}}{\rightleftharpoons} \underbrace{CH_3OH}_{\text{methanol}} + H_2O; \quad (1)$$

$$\Delta H \overset{\text{exo}}{=} -49.16\ \text{kJ mol}^{-1}$$

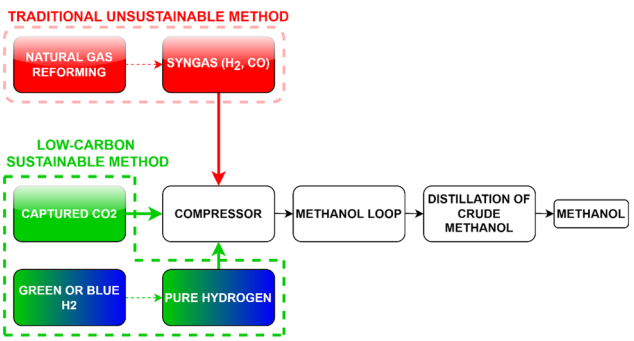


Fig. 8 Block diagram illustrating the traditional and renewable (pure $H_2$ with captured $CO_2$) methods of methanol production. Modified after ref. 76.

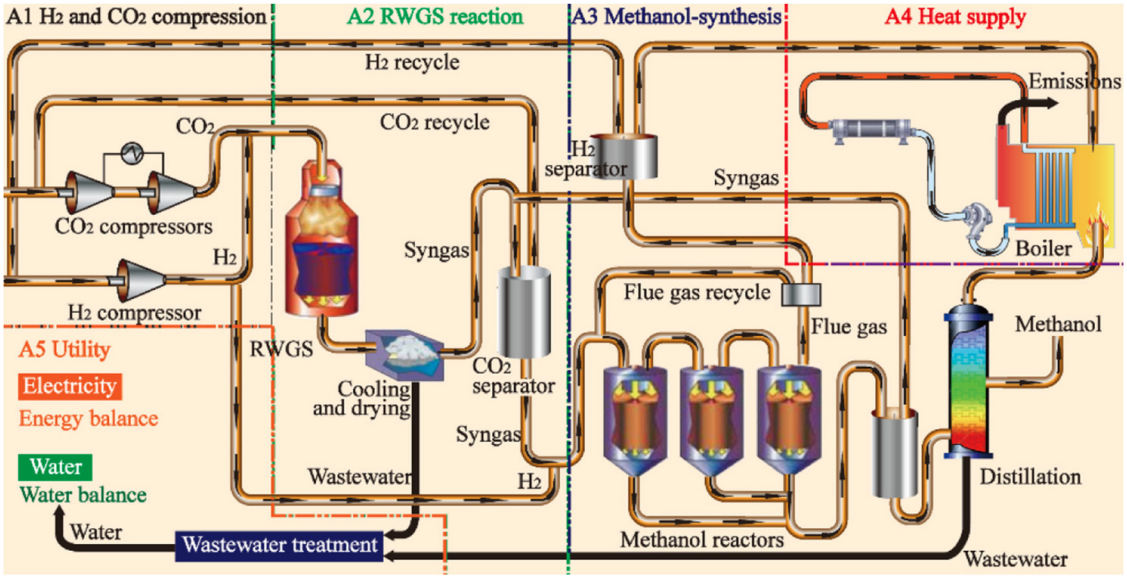


Fig. 9 Process flow diagram to produce e-methanol. From ref. 78.

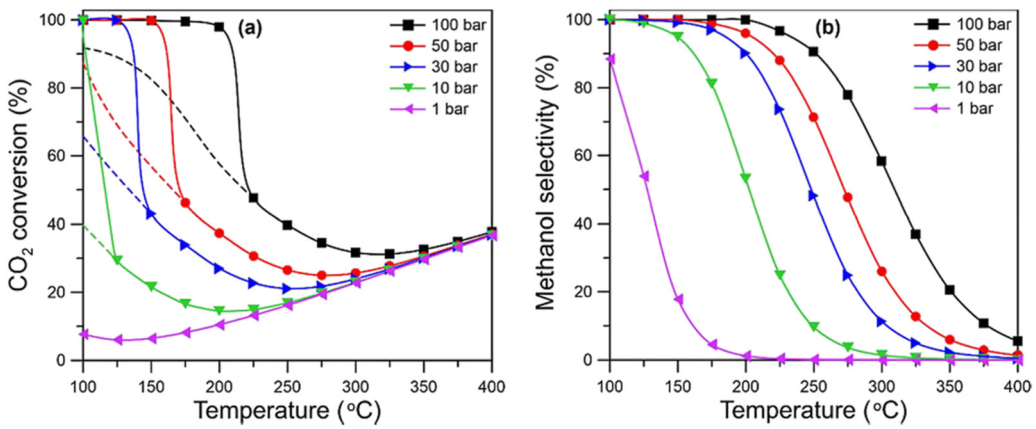


Fig. 10 Sensitivity of methanol synthesis (from $CO_2$ and $H_2$) as a function of pressure and temperature.[77,86]

Two-step process:

RWGS (600 °C, 24.5 bar[78]):

$$\underbrace{CO_2}_{\text{captured}} + \underbrace{H_2}_{\text{green or blue}} \overset{\text{catalyst}}{\rightleftharpoons} CO + H_2O; \quad (2)$$

$$\Delta H \overset{endo}{=} 41.22 \text{ kJ mol}^{-1} \ [\sim 600 - 900 \text{ °C}]$$

$$\underbrace{CO}_{\text{from RWGS}} + 2\underbrace{H_2}_{\text{green or blue}} \overset{\text{catalyst}}{\rightleftharpoons} \underbrace{CH_3OH}_{\text{methanol}}; \quad (3)$$

$$\Delta H \overset{exo}{=} -128 \text{ kJ mol}^{-1}$$

*2.4.1.3 Catalysts.* $CO_2$ is an inert gas due to its low reactivity (a stable molecule with a large bond dissociation energy of 1072 kJ $mol^{-1}$), and therefore it requires an active metal catalyst to promote its reaction with the $H_2$ to form methanol. An appropriate catalyst is important not only from the point of view of reaction performance, but also from an economic standpoint.[87] Traditionally, the catalysts that have been used for the synthesis of methanol are known to be found in abundance (*e.g.*, Cu, Zn, Al), but their tolerance to water is not robust, so significant water production in the synthesis of the e-methanol process reduces the activity (*e.g.*, through water adsorption, morphology changes, oxidation of the metal, *etc.*) and lifetime of the traditional catalysts.[77]

For e-methanol synthesis, catalysts exhibiting higher stability and activity in the presence of water are required for $CO_2$ hydrogenation. Various catalysts have been studied for the synthesis of e-methanol *via* heterogeneous catalysis, which range from transition metals/metal oxides to main group metals/metal oxides, particularly Cu-based, precious-metal-based, and metal oxides from main group elements.[88] Fig. 11 compares

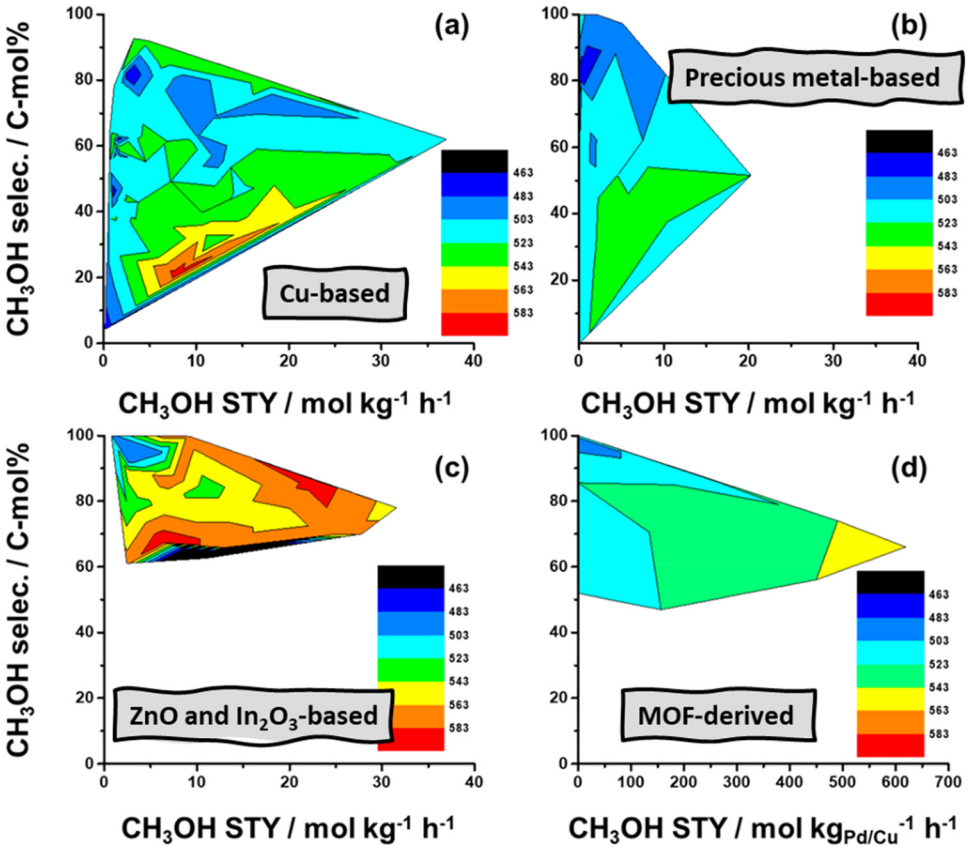


Fig. 11 Contour plots depicting catalytic performance in selectivity (conversion rate; in C-mol%) and space-time yield (STY; production rate; in mol $kg^{-1}$ $h^{-1}$) domain *versus* the reaction temperature (in K; color legend). The e-methanol production rate with MOF/ZIF-derived catalysts is normalized on active metals. Adapted from ref. 88.

four types of catalysts *via* contour plots showing catalytic performance in selectivity (conversion rate; in C-mol%) and space-time yield (STY; production rate; in mol $kg^{-1}$ $h^{-1}$) domain *versus* the reaction temperature (in K; color legend). Fig. 11 shows that Cu-based catalysts provide the largest production rate of e-methanol among all the catalysts (the rate with MOF/ZIF-derived catalysts is normalized on active metals). However, the selectivity of methanol decreases as the methanol production rate increases (*e.g.*, ~90 C-mol% to ~60 C-mol% for Cu-based catalysts). Although lower temperatures generally provide higher selectivity of methanol, it usually comes with a trade-off of lower production rates. Catalysts emerging recently, such as $In_2O_3$- and ZnO-based and MOF/ZIF-derived, have generally provided relatively high selectivity to methanol than Cu-based catalysts even with similar production rates, but they require relatively high operational temperature which translates to more energy input.[88] The performance of some of the catalysts presented in Fig. 11 have also been tested at a recent demonstration-scale e-methanol plant (FReSMe), which show similar observations as shown in Fig. 12.

Ruthenium (Ru)-based catalysts have been used to convert $CO_2$ to $CH_4$ (*e.g.*, *via* the Sabatier methanation process) with a selectivity between 99 and 100% over a range of operating temperatures, from a low of 60 °C to a high of ~450 °C.[90] Ru-based catalysts have been recently explored for their

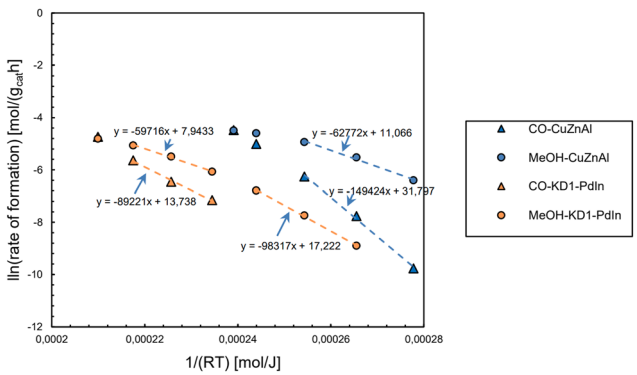


Fig. 12 Performance of selected catalysts in terms of the rate of production *versus* the input energy in the FReSMe project.[89]

potential in the synthesis of e-methanol from $H_2/CO_2$ and incorporating Ru with indium (In) has been shown to prevent methanation and instead produce methanol with >85% selectivity.[90] Other laboratory-scale advancements in preventing methanation include coating ruthenium with a thin layer of a porous plastic/polymer.[91,92]

In the case of a two-step process for e-methanol production that also includes a high-temperature RWGS reactor (usually the case, as shown in Fig. 9), barium zirconate-based perovskite-type catalysts doped with Y, Zn, and Ce show stable performance;[93]

particularly, $BaCe_{0.2}Zr_{0.6}Y_{0.16}Zn_{0.04}O_3$ has been used as a favorable candidate for the RWGS reaction according to recent studies.[78]

*2.4.1.4 Costs.* The minimum fuel selling price (MFSP; a price at which the net present value is zero) of methanol varies based on the cost of $H_2$ production, the cost of $CO_2$ as a feedstock, and the credit of saved $CO_2$ as shown in Fig. 13a. Fig. 13a shows that the average MFSP of e-methanol, compared to an average of \$0.38 per kg as the market price over the 2015–2020 period, varies between ~\$0.16 per kg and ~\$1.26 per kg depending on the cost of $H_2$ production (∈[\$0.8 per kg, \$5.0 per kg] with the base price as \$2 per kg), the cost of $CO_2$ as a feedstock (∈[\$17.3 per MT, \$38.6 per MT]), and the cost of saved carbon that can be traded (∈[\$0 per MT, \$200 per MT]) as a credit.[78] The feedstock costs of $CO_2$ assumed in Fig. 13a are \$17.3 per MT, \$20.6 per MT, and \$38.6 per MT for the methanol–ethanol coproduction, methanol–ammonia coproduction, and stand-alone methanol production systems, respectively.[78] For the MFSP of e-methanol to equal the market average over 2015–2020 (\$0.38 per kg), the breakeven costs of $H_2$ production with $CO_2$ credit (of \$200 per metric ton (MT)) and without $CO_2$ credit are estimated to be within \$2.09–2.24 per kg and \$0.77–0.95 per kg, respectively. By some estimates,[94–96] 65% of the total methanol production cost is the cost of producing renewable $H_2$. The estimated results in Fig. 13a are for a

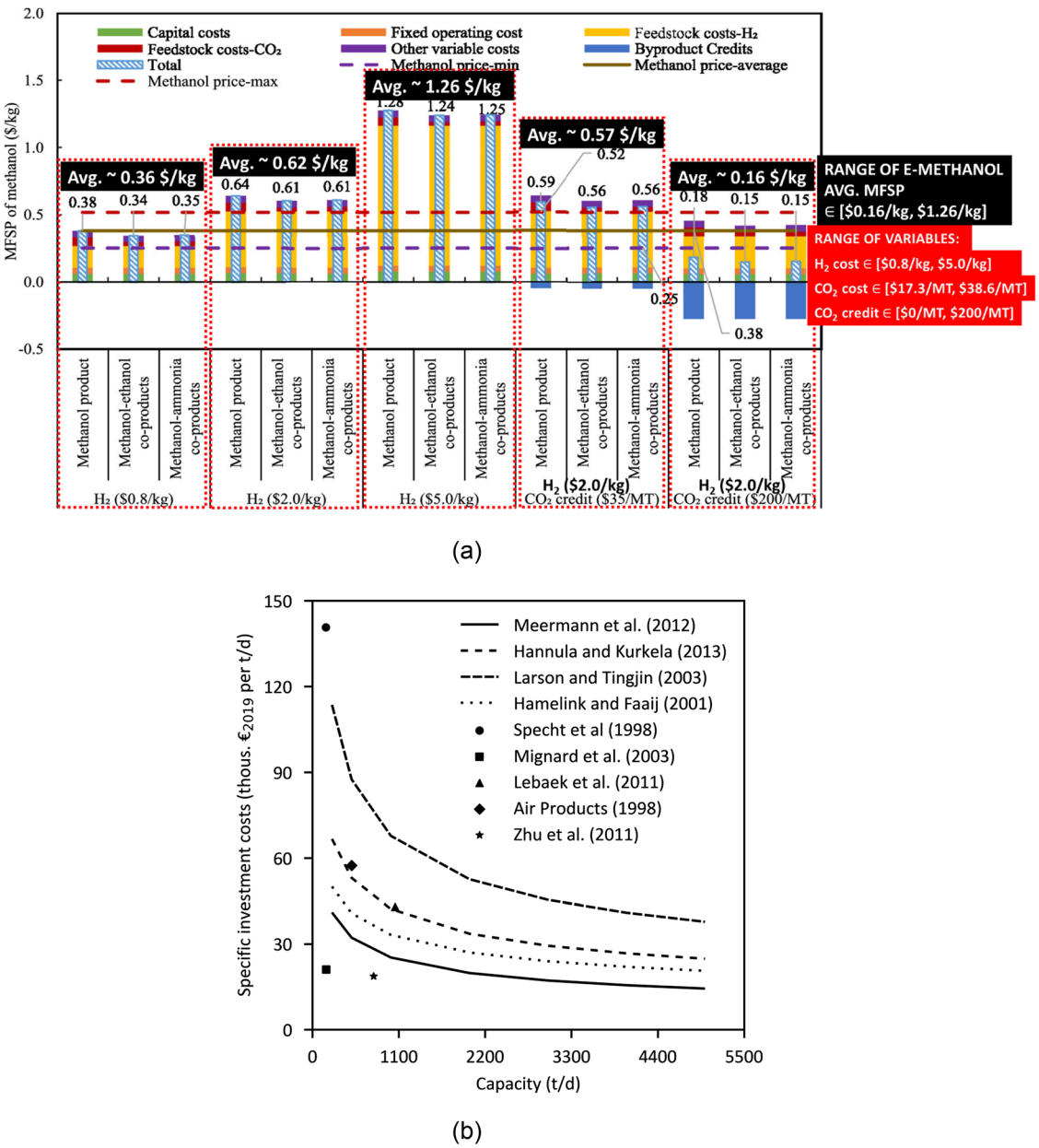


Fig. 13 (a) MFSP of e-methanol as a function of the $H_2$ production cost, $CO_2$ cost, and the credit for saved carbon, for a production capacity of 1190 MT per day. Adapted from ref. 78. (b) Cost of e-methanol production *versus* production plant capacity. From ref. 97.

production capacity of 1190 MT per day,[78] whereas based on the results of several studies,[97] as shown in Fig. 13b, the cost of e-methanol production decreases with increasing capacity until and beyond 4400 t per day.

**2.4.2 e-Kerosene/sustainable aviation fuel (SAF) production.** Carbon emissions from aviation account for ~2–3% of global carbon emissions, and the emissions from air travel continue to grow rapidly. One possible solution to reduce emissions from the aviation sector is through the use of sustainable aviation fuel (SAF), which is the name given to the synthetic aviation fuels produced using clean $H_2$ and captured $CO_2$. Besides being a carbon-neutral fuel, a major practical advantage of SAF is that it can be blended with the conventional fossil fuel-based aviation fuel with no infrastructure or equipment changes. The first commercial use of SAF was in a Boeing 737 passenger service flight on February 8, 2021, from Amsterdam to Madrid, which carried 500 liters of e-kerosene mixed with a fossil fuel-based regular aviation fuel.

*2.4.2.1 Process.* SAF can be produced using the Fischer–Tropsch (FT) process, which is a heterogeneously catalyzed process to convert $CO_2/H_2$ and syngas ($CO/H_2$) to liquid hydrocarbons (*e.g.*, e-diesel/e-kerosene) with the desired composition (carbon chain and length) based on the process/operating conditions. The composition of the SAF consists of *n*-alkanes, iso-alkanes, and cycloalkanes, with a typical carbon chain length distribution ranging from C8 to C18.[98] The SAF production *via* FT synthesis includes six process areas, which are (i) $H_2$ and $CO_2$ compression, (ii) RWGS reactor, (iii) FT synthesis reactor, (iv) hydro-processing, (v) power generation, and (vi) utility.[99] The FT synthesis takes place in a second reactor as it requires CO as the feedstock that is generated using $CO_2/H_2$ in the first reverse water gas shift reaction (RWGS) reactor.

Just like the synthesis of e-methanol, $H_2$ and $CO_2$ are pressurized/compressed (~25 bar) before feeding them into the first reactor that operates at high temperature and high pressure in case the initial pressures of the supplied $CO_2$ and $H_2$ are lower than the operating pressure of the reactor. The FT reaction is highly exothermic generating heat, which is supplied for the endothermic reaction in the RWGS reactor (Fig. 14).

A key factor that influences the FT synthesis is the efficient removal of heat from the reactor as FT reactions are highly exothermic which generate heat. The four commercially used designs of the FT synthesis reactor are based on different heat transfer mechanisms, which include[100] (i) the circulating fluidized bed reactor, (ii) the fluidized bed reactor, (iii) the tubular fixed bed reactor, and (iv) the slurry phase reactor.

*2.4.2.1.1 $H_2$ and $CO_2$ utilization.* Based on the FT process flow diagram shown in Fig. 14, producing a kg of SAF requires an estimated ~1.36 kg $H_2$ and 14.55 kg $CO_2$,[99] with Co- and Fe-based catalysts for the FT synthesis and $BaCe_{0.2}Zr_{0.6}Y_{0.16}Zn_{0.04}O_3$ as the catalyst for the RWGS reaction. Few other studies[82,83,101] mention the net $CO_2$ utilization in the FT process as 2.6 t $CO_2$ per 1t of liquid FT fuel (or equivalently, a kg of FT fuel requires 2.6 kg of $CO_2$), but these estimates are for the traditional FT fuel (*versus* the synthetic FT fuel) that is produced using $CO_2$ and methane reforming.[101]

*2.4.2.2 Reactions.* The main FT reaction (eqn (4)) requires CO as the feedstock, which is generated from the captured $CO_2$ *via* the RWGS reaction of $H_2$ and $CO_2$ (eqn (5)).

FT reaction for e-diesel:

$$n\mathrm{CO} + (2n+1)\underbrace{\mathrm{H_2}}_{\text{green or blue}} \overset{\text{catalyst}}{\rightleftharpoons} \mathrm{C}_n\mathrm{H}_{2n+2} + n\mathrm{H_2O}; \quad (4)$$

$$n \in [17, 32]; \quad \Delta H \overset{exo}{=} -x \text{ kJ mol}^{-1}$$

RWGS (600 °C, 24.5 bar[99]):

$$\underbrace{\mathrm{CO_2}}_{\text{captured}} + \underbrace{\mathrm{H_2}}_{\text{green or blue}} \overset{\text{catalyst}}{\rightleftharpoons} \mathrm{CO} + \mathrm{H_2O}; \quad (5)$$

$$\Delta H \overset{endo}{=} 41.22 \text{ kJ mol}^{-1} \; [\sim 600 - 900\ ^\circ\mathrm{C}]$$

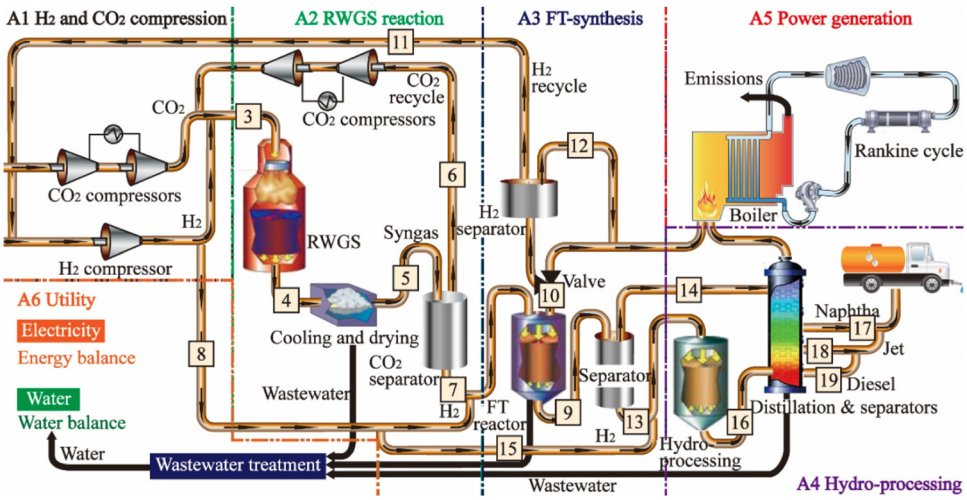


Fig. 14 Process flow diagram to produce a high-density liquid e-fuel (*e.g.*, SAF) *via* the Fischer–Tropsch (FT) process. From ref. 99.

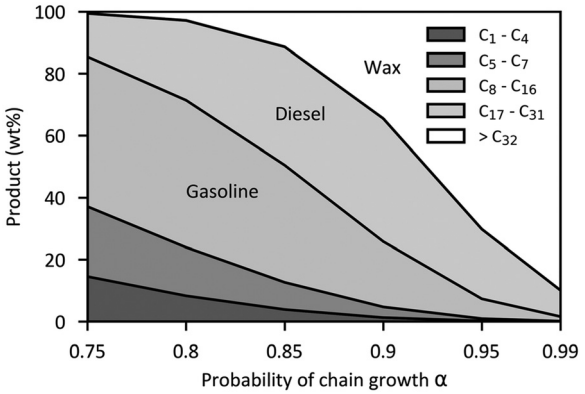


Fig. 15 Probabilistic distribution of the hydrocarbon products with different carbon chain lengths in the Fischer–Tropsch (FT) process.[97]

The probabilistic distribution of the carbon chain length in the FT synthesis is described by the Anderson–Schulz–Flory distribution, which is mathematically expressed in eqn (6) and graphically illustrated in Fig. 15. The parameters $W_n$, $n$, and $\alpha$ in eqn (6) represent the weight fraction of the hydrocarbon product, the carbon chain length of the hydrocarbon product, and the growth probability of the carbon chain, respectively. The probability of the carbon chain ($\alpha$) with length $n$ is a function of the catalysts used in the FT process, plus the composition of the syngas and the operating conditions.[97] The SAF produced using the FT process is typically liquid products with 17–32 carbon atoms per chain. As shown in Fig. 15, there are various lengths of carbon chains produced in the FT process whose relative weights are a function of the chain growth probability. Other non-diesel products produced *via* FT are converted to diesel *via* upgrading, which primarily involves hydrocracking of waxes according to eqn (7).

$$W_n = n(1-\alpha)^2\alpha^{n-1} \quad (6)$$

$$\text{Wax} + \underbrace{H_2}_{\text{green or blue}} \overset{\text{catalyst}}{\rightleftharpoons} C_nH_{2n+2}; \quad (7)$$

*2.4.2.3 Catalysts.* Traditionally, Co- and Fe-based catalysts have been used for commercial-scale FT processes, whereas precious metal-based catalysts (*e.g.*, nickel- and ruthenium-based) that are catalytically more active do not yet find a practical role in industrial applications.[97] Other relevant catalysts like porous metal oxides (*e.g.*, zeolite and aluminum oxide) with large specific surfaces are used as carriers for the catalyst. The use of Co-based catalysts is limited to operating conditions with relatively low temperatures (200–240 °C), but the Fe-based catalyst can be used over a wider range of operating temperatures ranging from low (200–240 °C) to high (300–360 °C).[99] Recent laboratory-scale advancements in catalysts for FT synthesis include combining Fe-based catalysts with transition metal promoters (*e.g.*, Fe–Mn–K) for high conversion rates and high selectivity to SAF;[102] the catalytic performance using the three transition metal promoters (Na-, K-, and Cs-based) was found to

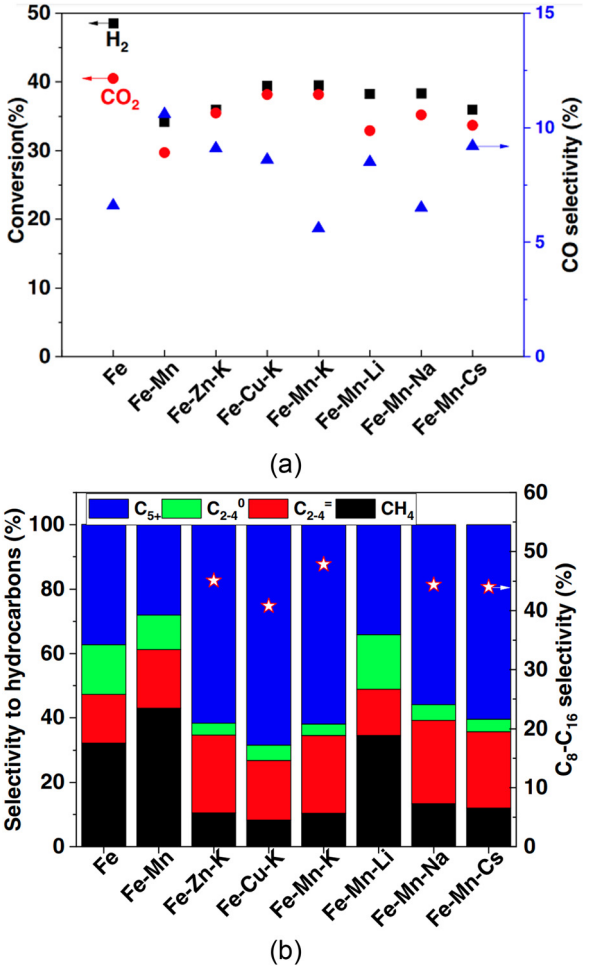


Fig. 16 Catalyst performance for the FT synthesis in terms of (a) the $CO_2$/$H_2$ conversion rate and (b) selectivity to hydrocarbons, especially longer-chain carbons (SAF). From ref. 102.

be similar, but the K-based metal promoter (Fe–Mn–K catalyst) showed high $CO_2/H_2$ conversion rates (Fig. 16a) and higher selectivity in longer-chain hydrocarbons (47.8% for C8–C16) than the selectivity from Na- and Cs-based metal promoters (44.4% and 44.0%, respectively) as shown in Fig. 16b.

*2.4.2.4 Costs.* The variation in the MFSP of FT fuel (SAF) with the cost of $H_2$ production, the cost of $CO_2$ as a feedstock, and the credit of saved $CO_2$ capture is shown in Fig. 17. Fig. 17 shows that the average MFSP of SAF varies between ~$4.30 per gal and ~$6.78 per gal depending on the cost of $H_2$ production (∈[$0.8 per kg, $5.0 per kg] with the base price as $2 per kg), the cost of $CO_2$ as a feedstock (∈[$0 per MT, $76.2 per MT] with the base price as $17.3 per MT), and the cost of saved carbon that can be traded (∈[$0 per MT, $300 per MT] with the base price as $0 per MT) as a credit.[99] The lowest MFSP (low-cost production) of FT fuel is potentially possible when the $CO_2$ is sourced from the ethanol, ethylene oxide, and ammonia plants, whereas the highest MFSP is potentially when the $CO_2$ is sourced from the hydrogen industry.[99] Besides the cost of $H_2$, $CO_2$, and $CO_2$ credit, the dominant parameters that have a major impact on

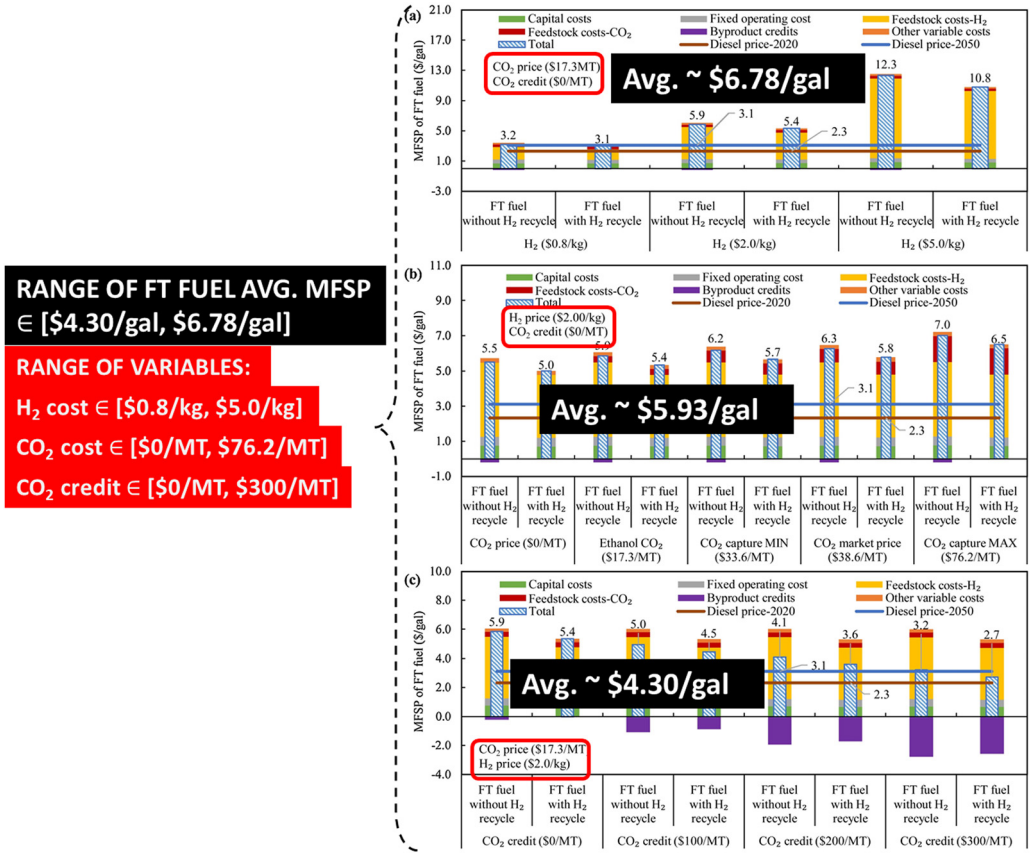


Fig. 17 MFSP of SAF (FT fuel) as a function of the $H_2$ production cost, $CO_2$ cost, and the credit for saved carbon for a production capacity of 351 MT per day (divided among 90 MT per day of naphtha, 164 MT per day of jet fuel, and 97 MT per day of diesel). Adapted from ref. 99.

the MFSP of FT fuel are the $H_2$ recycle ratio, CO conversion ratio of the FT reaction, and the $CO_2$ recycle ratio.[99] The estimated results in Fig. 17 are for a FT fuel production capacity of 351 MT per day (351 MT per day divided among 90 MT per day of naphtha, 164 MT per day of jet fuel, and 97 MT per day of diesel).[99]

# 3 Projects

The number of currently operational e-methanol and SAF production plants around the world is very few, where almost all these plants are at the pilot- or demonstration-scale, but many new commercial-scale plants are currently under development and many new plants are being announced. Table 6 summarizes the projects for commercial production of e-methanol and SAF projects that are described ahead in detail.

## 3.1 e-Methanol production

Four renewable methanol plants discussed below are the Harun Oni project in Chile, e-CO2Met project in Germany, MefCO2 in Germany, and George Olah plant (also called CRI) in Iceland.

**3.1.1 George Olah Plant, Svartsengi, Iceland (2012).** George Olah (GO) plant, operated by Carbon Recycling International (CRI), is an industrial-scale e-methanol facility, shown in Fig. 18, with a production capacity of 4000 tpa,[76] which uses the 5600 tpa of $CO_2$[103] captured from a nearby geothermal power plant and 800 tpa (1200 N $m^3$ $h^{-1}$) of $H_2$[103] produced through an alkaline electrolyzer run on renewable grid electricity.

**3.1.2 MefCO2, Niederaussem, Germany (2019).** This pilot-scale MefCO2 (methanol fuel from $CO_2$) plant, shown in Fig. 19, is one of the largest e-methanol synthesis plants in the European Union and uses 1.5 tpd of captured $CO_2$ from a coal (lignite)-fired power plant along with 1.5 tpd of $H_2$ from a 600 kW PEM electrolyzer (from Hydrogenics/Cummins) to produce 1 tpd (500 tpa capacity) of methanol.

**3.1.3 e-CO2Met Project, Leuna, Germany (2021).** TotalEnergies is the largest producer of conventional methanol in Europe, producing ~700 000 tpa of conventional methanol using fossil fuels at its refinery in Leuna, Germany. In 2019, TotalEnergies invested €150 MM in its refinery at Leuna with an aim to reduce the production of heavy products due to its decreasing demand, and increase the production of methanol which is one of the key raw materials in the chemical industry. TotalEnergies is partnering with Sunfire (Germany-based electrolyzer manufacturer) and Fraunhofer CBP (Germany-based biotech and sustainable chemistry research institute) to produce 1.5 tpd[105] of e-methanol *via* green $H_2$ produced from a 1 MW electrolyzer (high-temperature SOEC technology with

Table 6 Summary of projects for commercial production of liquid e-methanol and SAF

| e-Fuel ↓ | Project name | Companies | Location | Date started | Material consumption info | | Production capacity |
|---|---|---|---|---|---|---|---|
| | | | | | $H_2$ | $CO_2$ | |
| e-Methanol | George Olah Plant | Carbon Recycling International (CRI) | Svartsengi, Iceland | 2012 | 800 tpa (1200 N $m^3$ $h^{-1}$) produced using an alkaline electrolyzer powered by renewable energy | 5600 tpa captured from a nearby geothermal power plant | 4000 tpa |
| | MefCO2 | Consortium of 9 partners funded by the EU | Niederaussem, Germany | 2021 | 1.5 tpd from a 600 kW PEM electrolyzer from Cummins | 1.5 tpd of captured $CO_2$ from a coal (lignite)-fired power plant | 1 tpd (500 tpa capacity) |
| | e-CO2Met | TotalEnergies | Leuna, Germany | 2021 | 1 MW electrolyzer (high-temperature SOEC with 80% efficiency, from Sunfire) | Captured from TotalEnergies' refinery in Leuna | 1.5 tpd |
| | FReSMe | Consortium of 13 partners funded by the EU | Luleå, Sweden | 2021 | 100 N $m^3$ $h^{-1}$ recovered from the blast furnace in addition to production by electrolysis | 14 tpd captured from an industrial steel blast furnace | 1 tpd (2.5 tpd capacity) |
| | Haru Oni | Siemens Energy, Porsche, HIF, Enel, Exxon-Mobil, Gasco and ENAP | Punta Arenas, Chile | 2022 | 1.2 MW PEM electrolyzer (from Siemens Energy) powered by wind energy (3.4 MW Siemens Gamesa turbine) | DAC (from Global Thermostat) | ~750 000 liters in 2022 and 1 000 000 tons by 2026 |
| e-Kerosene (SAF) | Synthetic diesel plant | Velocys | Oklahoma City, USA | 2017 | — | — | 250 bpd |
| | atmosfair FairFuel | Solarbelt Fair-Fuel gGmbH | Werlte, Germany | 2021 | 160 tpa or 20.7 kg $h^{-1}$ using a 1.25 MW PEM electrolyzer powered by wind energy | DAC module and from waste valorization (biogas) | 350 tpa of synthetic crude oil |
| | Haru Oni | Siemens Energy, Porsche, HIF, Enel, Exxon-Mobil, Gasco and ENAP | Punta Arenas, Chile | 2022 | 1.2 MW PEM electrolyzer (from Siemens Energy) powered by wind energy (3.4 MW Siemens Gamesa turbine) | DAC (from Global Thermostat) | ~130 000, ~55 million, and ~550 million liters per year of e-gasoline[a] by the end of 2022, 2024, and 2026, respectively |
| | Bayou Fuels Plant | Velocys/OLCV | Natchez, Mississippi, USA | 2023 | — | — | 25 million gallons per year (35 million as capacity) |

[a] Haru Oni project uses the terms e-methanol and e-gasoline as two products, but it does not provide a separate number for e-kerosene, which is assumed to be part of e-gasoline.

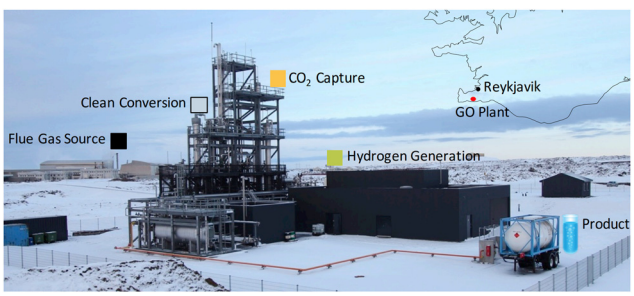


Fig. 18 CRI's GO plant in Svartsengi, Iceland, which uses $CO_2$ captured from the nearby geothermal power plant (in background) and $H_2$ produced through electrolysis to form renewable methanol. From ref. 103.

80% efficiency, from Sunfire) and $CO_2$ produced at TotalEnergies' refinery (in Leuna),[106] as shown in Fig. 20.

**3.1.4 FReSMe Project, Luleå, Sweden (2021).** FReSMe (From Residual Steel gases to Methanol) is a demonstration-scale project to produce e-methanol for ship transportation using $CO_2$ captured from an industrial steel blast furnace, and $H_2$ recovered from the blast furnace in addition to its production by electrolysis. The FReSMe project, shown in Fig. 21, used 14 tpd of $CO_2$ with 100 N $m^3$ $h^{-1}$ of $H_2$ from electrolysis to produce 1 tpd of e-methanol,[89] although the e-methanol production capacity of the plant is 2.5 tpd.[107]

**3.1.5 Haru Oni Project, Punta Arenas, Chile (expected by the end of 2022).** A group of companies (Siemens Energy, Porsche, HIF, Enel, ExxonMobil, Gasco and ENAP) led by HIF is building a plant to produce e-methanol in Chilean Patagonia using green $H_2$ and $CO_2$ captured from a DAC facility, which will produce ~750 000 litres (~350 tpa) of e-methanol in 2022 and later expanded to 1 000 000 tons by 2026.[75,108] This integrated plant (Fig. 22) will produce $H_2$ using a 1.2 MW PEM electrolyzer (from Siemens Energy) powered by 3.4 MW of wind energy (Siemens Gamesa turbine), which will be processed in a methanol synthesis reactor (Johnson Matthey's design) with

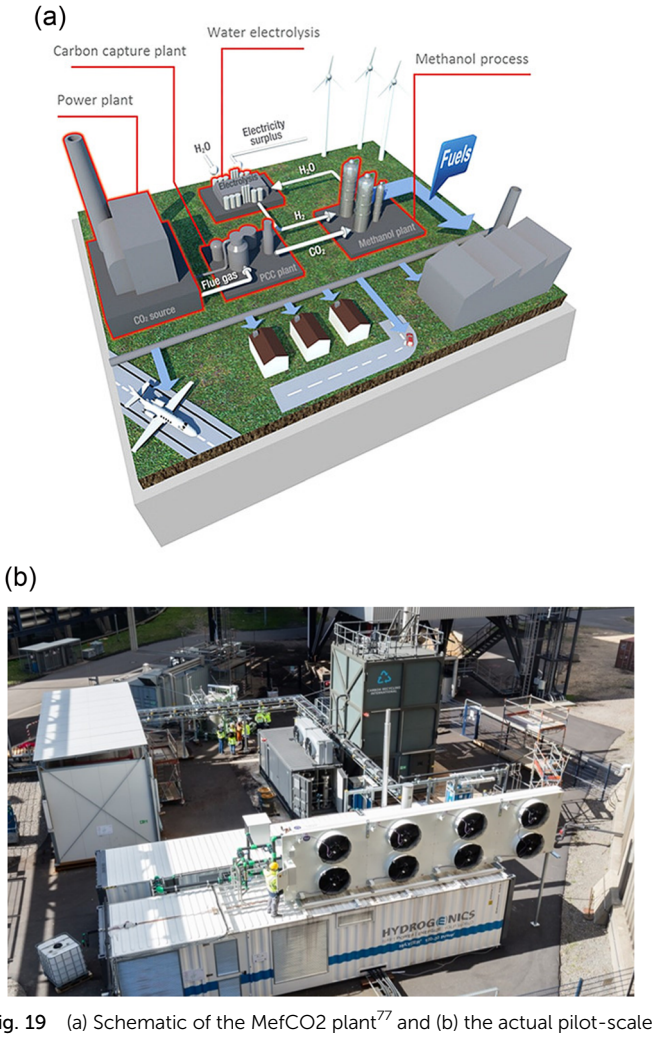


Fig. 19 (a) Schematic of the MefCO2 plant[77] and (b) the actual pilot-scale MefCO2 plant (right) at RWE's lignite-fired coal power plant in Niederaussem, Germany.[104]


Fig. 20 Schematic of the e-CO2Met Project, Leuna, which is scheduled to be fully operational after phase 2 which starts in 2022.

$CO_2$ captured from the air (from Global Thermostats) to produce e-methanol, and ~40% of the e-methanol will be converted to synthetic gasoline compatible with existing engines through a methanol to gasoline (MTG) plant located at the site

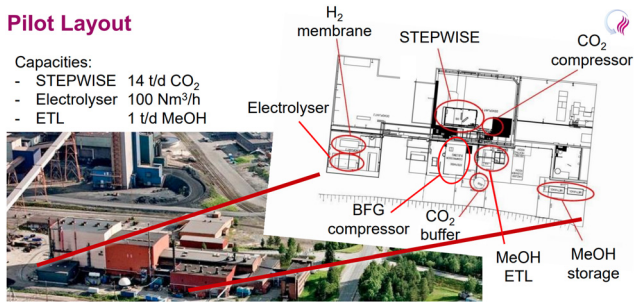


Fig. 21 Layout of the FReSMe project.[89]

(ExxonMobil's Technology). The carbon-neutral synthetic gasoline will be transported to Europe *via* a container ship, each having a loading capacity of 25 000–30 000 liters, to be used by Porsche and others for modern and classic sports cars.

**3.1.6 Other proposed projects.** Other projects that are under planning and/or development include[110] the following:

- Hy2Gen project in Germany with 61 000 tpa e-methanol production capacity. The $CO_2$ will be captured from a biogas plant and $H_2$ will be produced by electrolysis.
- A project in Norway by Swiss Liquid Future/Thyssenkrupp with 80 000 tpa e-methanol production capacity. The $CO_2$ will be captured from a ferrosilicon plant and $H_2$ will be produced by electrolysis powered by hydropower.
- A project in China by CRI and Jiangsu Sailboat Petrochemicals with 100 000 tpa e-methanol production capacity. The $CO_2$ and $H_2$ will be produced by electrolysis of water.
- A project in France by Vicat and Hynamics with 200 000 tpa e-methanol production capacity. The $CO_2$ will be captured from a cement plant and $H_2$ will be produced by electrolysis.

### 3.2 SAF production

Four renewable methanol plants discussed below are the Harun Oni project in Chile, e-CO2Met project in Germany, MefCO2 in Germany, and George Olah plant (also called CRI) in Iceland, respectively.

**3.2.1 Synthetic diesel plant, Oklahoma city, USA (2017).** The synthetic diesel plant at Oklahoma City[111] (Fig. 23a) demonstrated Velocys' Fischer–Tropsch technology through full commercial operation with 250 bpd of operational capacity.[112] This plant sold over 10 000 barrels of products (waxes, diesel and naphtha) to commercial off-takers and generated RIN credits under the Renewable Fuel Standard (RFS). This plant provided 1500+ hours data in enabling Velocys to scale its FT synthesis technology to other projects (*e.g.*, Mississippi Biorefinery and UK waste to jet projects). The $H_2$ was produced as syngas (an optimized mixture of carbon monoxide and hydrogen) by reforming natural gas, landfill gas, or by gasification of biomass or waste;[112] therefore, from the nomenclature perspective, SAF produced in this case could be referred to as bio-kerosene instead of e-kerosene.

Following a 20 month period of operation, a leak was identified at the ancillary coolant system of this plant which led to a reduction in its production capacity (a single reactor),

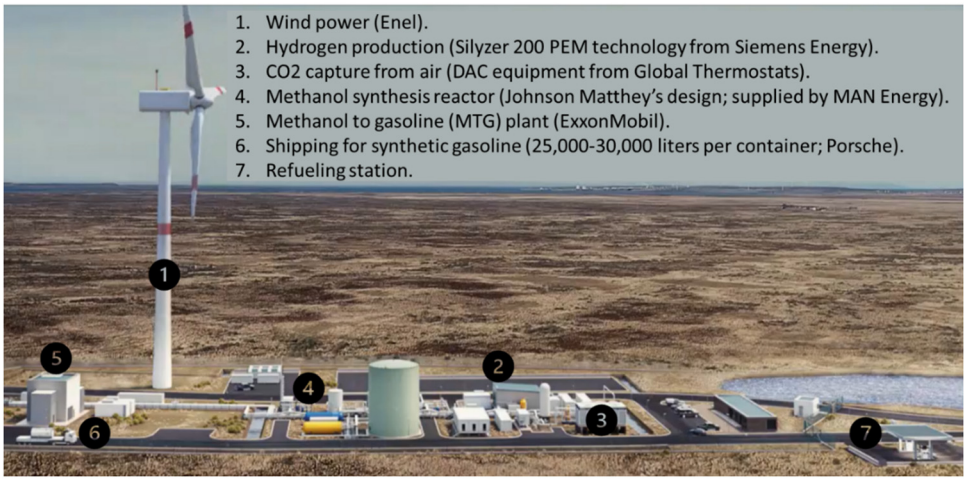


(a)

(b)

Fig. 22 (a) Schematic of the Haru Oni project, southern Chile, which will produce industrial-scale e-methanol starting from the end of 2022. Adapted from ref. 75. (b) Actual site of the Haru Oni project. From ref. 109.

and this subsequently resulted in closure of the plant due to accumulating effects, such as operating losses, not maintaining the specific requirements to generate RINs under the RFS pathway, *etc.*

**3.2.2 atmosfair FairFuel, Werlte, Germany (2021).** World's first commercial-scale plant to produce synthetic kerosene using $H_2$ and captured $CO_2$ started operations in October 2021 at Werlte, Germany, as shown in Fig. 24.[114,115] The plant (owned and operated by Solarbelt FairFuel gGmbH; Lufthansa Group is a pilot customer) produces 350 tpa of synthetic crude oil through Fischer–Tropsch synthesis from carbon monoxide (recovered from $CO_2$) and $H_2$, where synthetic crude oil is used to manufacture climate-neutral kerosene meant for aviation. The $H_2$ is produced using a 1.25 MW PEM electrolyzer (160 tpa or 20.7 kg $h^{-1}$ of $H_2$) powered by wind energy, while the $CO_2$ is captured using a DAC module and from waste valorization (biogas).

**3.2.3 Bayou Fuels Plant, Natchez, Mississippi, USA (expected by the end of 2023).** Velocys is using the experience gained through its Oklahoma City plant (U.S.) in developing a similar larger-scale (Fig. 25) FT gas-to-liquid plant (Bayou Fuels plant) at Natchez, Mississippi, US, in partnership with Oxy Low Carbon Ventures (OLCV).[116] This plant will use 3000 tons of woody biomass as the feedstock to produce 25 million gallons of SAF (with 35 million gallons per year of capacity) plus renewable naphtha. The SAF production capacity of this plant will be the largest capacity in the U.S. by the time it comes online in 2023, and it is also cited by the U.S. Federal Government as one

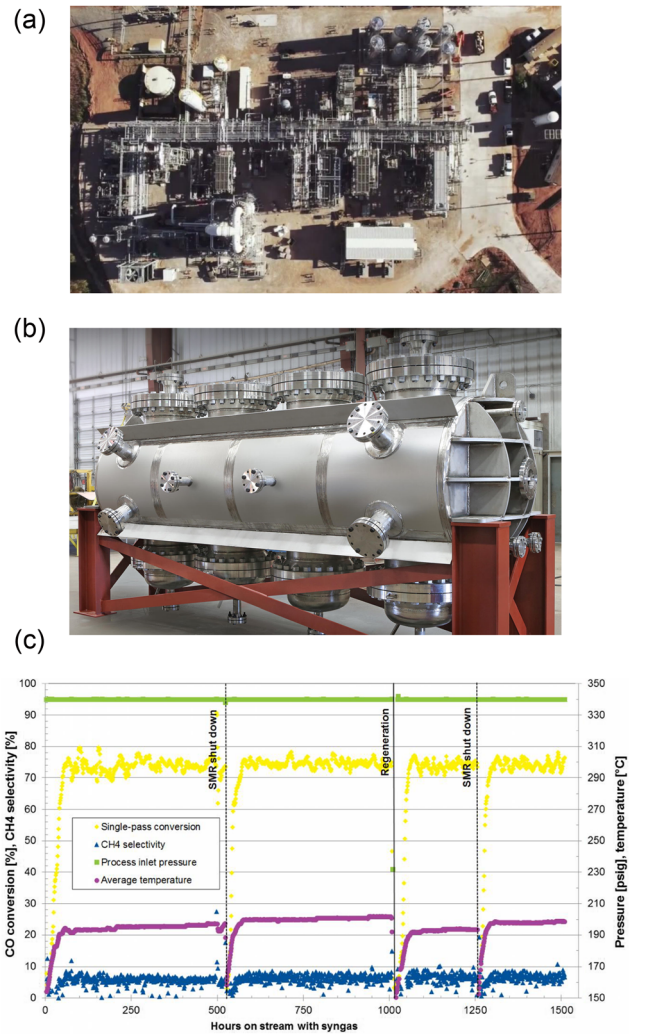


Fig. 23 (a) Velocys' first FT gas-to-liquid technology plant at Oklahoma City, US. From ref. 113. (b) Image of Velocys' FT reactor for the synthesis of hydrocarbons, particularly the SAF. (c) ~1500 hours of operational data from Velocys' synthetic diesel plant. From ref. 113.

Fig. 24 Actual site of the 350 tpa of SAF production plant at Werlte in Germany, including the electrolysis system that forms the core of the plant.[114,115]

of the projects that will help achieve the 2030 goal of producing at least 3 billion gallons per year of SAF in the U.S.

**3.2.4 Haru Oni Project, Punta Arenas, Chile (expected by the end of 2022).** This plant will also produce SAF in addition to

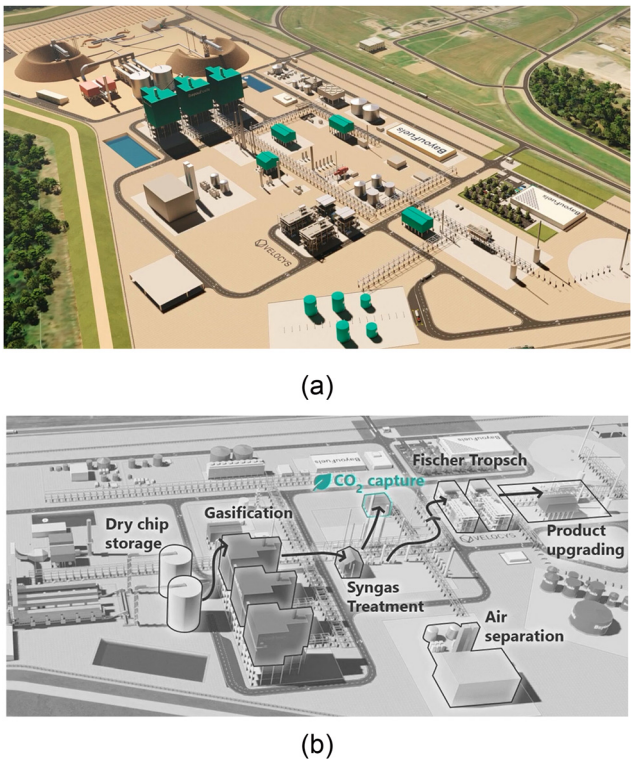


Fig. 25 (a) Schematic of the site of Velocys' proposed FT gas-to-liquid plant (Bayou Fuels plant) at Natchez, Mississippi, US. From ref. 116. (b) Schematic showing the layout of the Bayou Fuels Plant. From ref. 116.

e-methanol (as discussed earlier). The plant's capacity will be incrementally increased to produce ~130 000, ~55 million, and ~550 million litres per year of e-gasoline by the end of 2022, 2024, and 2026, respectively. The project does not provide a separate number for e-kerosene, which is assumed to be part of e-gasoline.

**3.2.5 Other proposed projects.** Other projects that are under planning and/or development include the following:

• A project development start-up called Synkero is developing a commercial-scale (50 000 tpa) plant at the Port of Amsterdam for the production of SAF using green $H_2$ and $CO_2$ which is scheduled to be completed in 2027. The Port of Amsterdam has an existing pipeline that supplies kerosene to Schiphol Airport.[117,118] The e-kerosene production plant will be powered by a 200 MW electrolysis system driven by wind energy (30 offshore turbines) which will produce 25 000 tpa of $H_2$, which will be processed with 200 000 tpa of captured $CO_2$ to produce 50 000 tpa of e-kerosene.[118]

• A consortium called Zenid,[119] comprising the Rotterdam airports (RTHA, RHIA), a sustainable air fuel (SAF) company (SkyNRG), and a DAC manufacturing company (Climeworks), is investigating the construction of an industrial-scale demonstration plant in Rotterdam, the Netherlands, to produce SAF with $H_2$ produced using the co-electrolysis unit and $CO_2$ captured from the air through a modular Fischer–Tropsch reactor.

• Infinium (a low-carbon liquid fuel producer in the U.S.) and Denbury (an oil and gas operator in the U.S.) announced a

partnership to build an e-fuel facility in Brazoria County, Texas, which will convert green $H_2$ (from renewable power) and industrial-sourced $CO_2$ into SAF and diesel using Infinium's proprietary technology.[120] This facility is anticipated to use 1.5 MM tpa of $CO_2$ captured from industrial sources and transported by Denbury using its $CO_2$ pipeline infrastructure.

• ExxonMobil and Neste will supply 1.25 million liters of SAF blended with refined jet fuel to Changi Airport for Singapore Airlines and Scoot flights by the third quarter of 2022.[121]

• Oxy initiated a front-end engineering and design (pre-FEED) for a 100 million liter (26.4 million gallons) annual capacity plant in British Columbia, Canada, to produce ultra-low carbon fuel for air, marine, rail, and truck transportation in Canada. The plant will use Carbon Engineering's DAC technology to capture $CO_2$.[122]

• Norsk e-Fuel will build a SAF plant in Mosjøen, Norway, on a 24 000 $m^2$ large plot, which will use 100% renewable electricity to produce $H_2$ through electrolysis (from Sunfire) and capture $CO_2$ from air using Climeworks' DAC technology.[123] The plant's production capacity will be 12.5 million liters of SAF by 2024 and 25 million liters of SAF by 2026.

## 4 Outlook and recommendations

Although the current market for $CO_2$ utilization is relatively small and will not likely rise much in the short- to medium-term without a significant policy change that puts a competitive price on $CO_2$ emissions in major $CO_2$ emitting countries, one of the major sectors with a potential to drive the $CO_2$ utilization demand in the absence of a policy is the blending of e-methanol and SAF with fossil fuel-produced methanol and jet fuel/diesel, respectively. Unlike hydrogen as a fuel, these e-fuels are readily-compatible with existing internal combustion engines in aviation, shipping, freight, *etc.*, and do not require any changes to the handling and logistics infrastructure. The production of liquid e-fuels is energy intensive and requires significant quantities of both $H_2$ and $CO_2$, and arranging such a large supply of both $H_2$ and $CO_2$ to produce e-fuels at scale can be complex and challenging. The production costs for liquid e-fuels are also significantly higher than their fossil fuel-produced counterparts, primarily due to the costs involved in producing hydrogen. However, these holistic challenges must consider the following two incentives:

(1) Reaching net-zero by 2050 requires a relatively huge reduction in $CO_2$ compared to the current capture capacity, such that the 2030 target (800 MM tpa), and possibly the 2050 target, does not appear to be practically achievable. This implies that, due to the current under-capacity of CCUS and the large jump required to reach 800 MM tpa in less than a decade, the social and political pressure will ramp up as an alternative to not meeting the climate goals, which can suddenly lead to cost-prohibitive measures from various societal instruments, including government, law, *etc.* In this direction, a small but initial step has been taken by the recent U.S. Securities and Exchange Commission rule which enhanced the monitoring requirements for reporting Scope 1, Scope 2, and Scope 3 emissions, enforcing which did not require any new or exclusive law. The oil and gas companies that are already taking steps to decarbonize their value chain will be in a much better position to face these challenges.

(2) $CO_2$ utilization is not an alternative to the large-scale $CO_2$ storage required for reductions in $CO_2$ emissions, but it can still support the goal of reducing the emissions. Cultivating an early opportunity in $CO_2$ utilization through the production of liquid e-fuels will not only help create partnerships required to secure $CO_2$ supply chains, it can also lead to new markets for carbon-neutral liquid e-fuels that can be simply blended with their fossil fuel-based counterparts.

## Author contributions

Harpreet Singh: conceptualization, investigation, project administration, writing – original draft preparation, writing – review and editing. Chengxi Li: project administration, writing – review and editing. Peng Cheng: funding acquisition, resources, supervision. Xunjie Wang: funding acquisition, resources, supervision. Qing Liu: writing – review and editing.

## Conflicts of interest

There are no conflicts to declare.

## Acknowledgements

The authors would like to acknowledge the useful discussions with colleagues from CNPC USA and the support of CNPC's Beijing office, especially Mr Xu Wang, Mr Yuxin Wang, Mr Zhenzhou Yang, Dr Chunyan Qi, and Mr Fuchen Liu.

## References

1 Auguste and others, Mission Possible: Reaching net-zero carbon emissions from harder-to-abate sectors, 2018, **https://www.energy-transitions.org/publications/mission-possible/**.

2 IEA, Energy Technology Perspectives 2020, 2020, p. 174. **https://iea.blob.core.windows.net/assets/181b48b4-323f-454d-96fb-0bb1889d96a9/CCUS_in_clean_energy_transitions.pdf**, DOI: **10.1787/d07136f0-en**.

3 N. Adomaitis and J. Harvey, *Global climate goals 'virtually impossible' without carbon capture – IEA*, Reuters, 2020.

4 G. Hering and B. Montgomery, *First major US hydrogen-burning power plant nears completion in Ohio*, S&P Global Platts Media, 2021.

5 IEA, *Putting $CO_2$ to Use: Creating value from emissions*, 2019, **https://www.iea.org/reports/putting-co2-to-use**, DOI: **10.1787/dfeabbf4-en**.

6 C. Hobson and C. Márquez, Renewable methanol report, 2018, pp. 1–26.

7 CAPA, Aviation Sustainability and the Environment, CAPA 23-Jun-2022|CAPA, CAPA – Centre for Aviation, 2022.
8 M. Kayfeci, A. Keçebaş and M. Bayat, Hydrogen production, in *Solar Hydrogen Production*, ed. F. Calise, M. D.D'Accadia, M. Santarelli, A. Lanzini and D. Ferrero, Academic Press, 2019, ch. 3, pp. 45–83, DOI: 10.1016/B978-0-12-814853-2.00003-5.
9 N. Sazali, Emerging technologies by hydrogen: A review, *Int. J. Hydrogen Energy*, 2020, **45**, 18753–18771.
10 M.-K. Kazi, F. Eljack, M. M. El-Halwagi and M. Haouari, Green hydrogen for industrial sector decarbonization: Costs and impacts on hydrogen economy in qatar, *Comput. Chem. Eng.*, 2021, **145**, 107144.
11 U.S. DOE, *Hydrogen Program Plan*, 2020, https://www.hydrogen.energy.gov/pdfs/program_plan2011.pdf.
12 H. Nazir, *et al.*, Is the $H_2$ economy realizable in the foreseeable future? Part I: $H_2$ production methods, *Int. J. Hydrogen Energy*, 2020, **45**, 13777–13788.
13 F. Elmanakhly, *et al.*, Hydrogen economy transition plan: A case study on Ontario, *AIMSE*, 2021, **9**, 775–811.
14 C. M. Kalamaras and A. M. Efstathiou, Hydrogen Production Technologies: Current State and Future Developments, *Conf. Pap. Energy*, 2013, e690627.
15 R. Pinsky, P. Sabharwall, J. Hartvigsen and J. O'Brien, Comparative review of hydrogen production technologies for nuclear hybrid energy systems, *Prog. Nucl. Energy*, 2020, **123**, 103317.
16 H. Thomas, *et al.*, *Options for producing low-carbon hydrogen at scale*, The Royal Society, 2018.
17 N. Sánchez-Bastardo, R. Schlögl and H. Ruland, Methane Pyrolysis for Zero-Emission Hydrogen Production: A Potential Bridge Technology from Fossil Fuels to a Renewable and Sustainable Hydrogen Economy, *Ind. Eng. Chem. Res.*, 2021, **60**, 11855–11881.
18 P. R. Kapadia, M. Kallos, L. Chris and I. D. Gates, Potential for Hydrogen Generation during In Situ Combustion of Bitumen, OnePetro, 2009, DOI: 10.2118/122028-MS.
19 T. Jacobs, *Canadian Operator Works To Transform an Oil Field Into a Hydrogen Factory*, SPE JPT, 2021.
20 A. Akhtar, V. Krepl and T. Ivanova, A Combined Overview of Combustion, Pyrolysis, and Gasification of Biomass, *Energy Fuels*, 2018, **32**, 7294–7318.
21 V. Singh and D. Das, Chapter 3 – Potential of Hydrogen Production From Biomass, in *Science and Engineering of Hydrogen-Based Energy Technologies*, ed. P. E. V. de Miranda, Academic Press, 2019, pp. 123–164, DOI: 10.1016/B978-0-12-814251-6.00003-4.
22 V. Zgonnik, The occurrence and geoscience of natural hydrogen: A comprehensive review, *Earth-Sci. Rev.*, 2020, **203**, 103140.
23 V. Zgonnik, *et al.*, Evidence for natural molecular hydrogen seepage associated with Carolina bays (surficial, ovoid depressions on the Atlantic Coastal Plain, Province of the USA), *Prog. Earth Planetary Sci.*, 2015, **2**, 1–15.
24 S. P. Gregory, M. J. Barnett, L. P. Field and A. E. Milodowski, Subsurface Microbial Hydrogen Cycling: Natural Occurrence and Implications for Industry, *Microorganisms*, 2019, **7**, 53.
25 J. Guélard, *et al.*, Natural $H_2$ in Kansas: Deep or shallow origin?, *Geochem., Geophys., Geosyst.*, 2017, **18**, 1841–1865.
26 A. Prinzhofer, C. S. Tahara Cissé and A. B. Diallo, Discovery of a large accumulation of natural hydrogen in Bourakebougou (Mali), *Int. J. Hydrogen Energy*, 2018, **43**, 19315–19326.
27 S. L. Worman, L. F. Pratson, J. A. Karson and W. H. Schlesinger, Abiotic hydrogen ($H_2$) sources and sinks near the Mid-Ocean Ridge (MOR) with implications for the subseafloor biosphere, *Proc. Natl. Acad. Sci. U. S. A.*, 2020, **117**, 13283–13293.
28 R. M. Coveney, Jr., E. D. Goebel, E. J. Zeller, G. A. M. Dreschhoff and E. E. Angino, Serpentinization and the Origin of Hydrogen Gas in Kansas, *AAPG Bull.*, 1987, **71**, 39–48.
29 E. D. Goebel, R. M. Coveney, Jr, E. E. Angino and E. Zeller, Naturally Occurring Hydrogen Gas from a Borehole on the Western Flank of Nemaha Anticline in Kansas, *AAPG Bull.*, 1983, **67**, 1324.
30 A. Kovač, M. Paranos and D. Marciuš, Hydrogen in energy transition: A review, *Int. J. Hydrogen Energy*, 2021, **46**, 10016–10035.
31 S. A. Grigoriev, V. N. Fateev, D. G. Bessarabov and P. Millet, Current status, research trends, and challenges in water electrolysis science and technology, *Int. J. Hydrogen Energy*, 2020, **45**, 26036–26058.
32 A. Morozov, Comparative Analysis of Hydrogen Production Methods with Nuclear Reactors, 2008.
33 R. Perret, Solar Thermochemical Hydrogen Production Research (STCH) Thermochemical Cycle Selection and Investment Priority, 2011, https://www.osti.gov/biblio/1671699-solar-thermochemical-hydrogen-production-research-stch-thermochemical-cycle-selection-investment-priority.
34 A. Boretti, Technology Readiness Level of Solar Thermochemical Splitting Cycles, *ACS Energy Lett.*, 2021, **6**, 1170–1174.
35 F. Safari and I. Dincer, A review and comparative evaluation of thermochemical water splitting cycles for hydrogen production, *Energy Convers. Manage.*, 2020, **205**, 112182.
36 U.S. DOE, DOE Technical Targets for Hydrogen Production from Thermochemical Water Splitting, 2021, https://www.energy.gov/eere/fuelcells/doe-technical-targets-hydrogen-production-thermochemical-water-splitting.
37 U.S. DOE, DOE Technical Targets for Hydrogen Production from Photoelectrochemical Water Splitting, 2021, https://www.energy.gov/eere/fuelcells/doe-technical-targets-hydrogen-production-photoelectrochemical-water-splitting.
38 U.S. DOE, DOE Technical Targets for Hydrogen Production from Electrolysis, 2021, https://www.energy.gov/eere/fuelcells/doe-technical-targets-hydrogen-production-electrolysis.
39 M. Bui, *et al.*, Carbon capture and storage (CCS): the way forward, *Energy Environ. Sci.*, 2018, **11**, 1062–1176.
40 S. W. Nam, S. P. Yoon, H. Y. Ha, S.-A. Hong and A. P. Maganyuk, Methane steam reforming in a Pd-Ru membrane reactor, *Korean J. Chem. Eng.*, 2000, **17**, 288–291.

41 J. Tong and Y. Matsumura, Effect of catalytic activity on methane steam reforming in hydrogen-permeable membrane reactor, *Appl. Catal., A*, 2005, **286**, 226–231.
42 M. Sarić, Y. C. van Delft, R. Sumbharaju, D. F. Meyer and A. de Groot, Steam reforming of methane in a bench-scale membrane reactor at realistic working conditions, *Catal. Today*, 2012, **193**, 74–80.
43 T. Kume, *et al.*, Performance evaluation of membrane on catalyst module for hydrogen production from natural gas, *Int. J. Hydrogen Energy*, 2013, **38**, 6079–6084.
44 B. Dittmar, *et al.*, Methane steam reforming operation and thermal stability of new porous metal supported tubular palladium composite membranes, *Int. J. Hydrogen Energy*, 2013, **38**, 8759–8771.
45 H. W. Abu El Hawa, S. N. Paglieri, C. C. Morris, A. Harale and J. Douglas Way, Application of a Pd–Ru composite membrane to hydrogen production in a high temperature membrane reactor, *Sep. Purif. Technol.*, 2015, **147**, 388–397.
46 H. W. Abu El Hawa, S.-T. B. Lundin, N. S. Patki and J. Douglas Way, Steam methane reforming in a PdAu membrane reactor: Long-term assessment, *Int. J. Hydrogen Energy*, 2016, **41**, 10193–10201.
47 B. Anzelmo, J. Wilcox and S. Liguori, Natural gas steam reforming reaction at low temperature and pressure conditions for hydrogen production *via* Pd/PSS membrane reactor, *J. Membr. Sci.*, 2017, **522**, 343–350.
48 C.-H. Kim, J.-Y. Han, H. Lim, D.-W. Kim and S.-K. Ryi, Methane steam reforming in a membrane reactor using high-permeable and low-selective Pd-Ru membrane, *Korean J. Chem. Eng.*, 2017, **34**, 1260–1265.
49 C.-H. Kim, *et al.*, Hydrogen production by steam methane reforming in a membrane reactor equipped with a Pd composite membrane deposited on a porous stainless steel, *Int. J. Hydrogen Energy*, 2018, **43**, 7684–7692.
50 IRENA, *Hydrogen: A renewable energy perspective*, 2019, **https://www.irena.org/publications/2019/Sep/Hydrogen-A-renewable-energy-perspective**.
51 J. Davies, F. Dolci, D. Klassek-Bajorek, R. Ortiz Cebolla and E. Weidner, Current status of Chemical Energy Storage Technologies, 2020, **https://publications.jrc.ec.europa.eu/repository/handle/JRC118776**.
52 R. Shaw and S. Mukherjee, The development of carbon capture and storage (CCS) in India: A critical review, *Carbon Capture Sci. Technol.*, 2022, 100036, DOI: **10.1016/j.ccst.2022.100036**.
53 A. I. Osman, M. Hefny, M. I. A. Abdel Maksoud, A. M. Elgarahy and D. W. Rooney, Recent advances in carbon capture storage and utilisation technologies: a review, *Environ. Chem. Lett.*, 2021, **19**, 797–849.
54 M. Zaman and J. H. Lee, Carbon capture from stationary power generation sources: A review of the current status of the technologies, *Korean J. Chem. Eng.*, 2013, **30**, 1497–1526.
55 N. S. Sifat and Y. Haseli, A Critical Review of $CO_2$ Capture Technologies and Prospects for Clean Power Generation, *Energies*, 2019, **12**, 4143.
56 O. Linjala, Review on post-combustion carbon capture technologies and capture of biogenic $CO_2$ using pilot-scale equipment, in Katsaus polton jälkeiseen hiilidioksidin talteenottoon kehitettyihin teknologioihin sekä bioperäisen hiilidioksidin talteenotto pilot-mittakaavan koelaitteistolla, Master's thesis, LUT University, 2021.
57 T. Lockwood, A Compararitive Review of Next-generation Carbon Capture Technologies for Coal-fired Power Plant, *Energy Procedia*, 2017, **114**, 2658–2670.
58 Y. Yamauchi and K. Akiyama, Innovative zero-emission coal gasification power generation project, *Energy Procedia*, 2013, **37**, 6579–6586.
59 J. Li, *et al.*, $CO_2$ Capture with Chemical Looping Combustion of Gaseous Fuels: An Overview, *Energy Fuels*, 2017, **31**, 3475–3524.
60 L.-S. Fan, L. Zeng, W. Wang and S. Luo, Chemical looping processes for $CO_2$ capture and carbonaceous fuel conversion – prospect and opportunity, *Energy Environ. Sci.*, 2012, **5**, 7254–7280.
61 S. Ferguson and A. Tarrant, Molten Carbonate Fuel Cells for 90% Post Combustion $CO_2$ Capture From a New Build CCGT, *Front. Energy Res.*, 2021, **9**, 359.
62 X. Zhang, Current status of stationary fuel cells for coal power generation, *Clean Energy*, 2018, **2**, 126–139.
63 Osaki CoolGen Corp, The Progress of Osaki CoolGen Project ~ Oxygen-blown Integrated Coal Gasification Fuel Cell Combined Cycle Demonstration Project, 2017.
64 T. M. Gür, Carbon Dioxide Emissions, Capture, Storage and Utilization: Review of Materials, Processes and Technologies, *Prog. Energy Combust. Sci.*, 2022, **89**, 100965.
65 S. Consonni, L. Mastropasqua, M. Spinelli, T. A. Barckholtz and S. Campanari, Low-carbon hydrogen *via* integration of steam methane reforming with molten carbonate fuel cells at low fuel utilization, *Adv. Appl. Energy*, 2021, **2**, 100010.
66 R. Barker, Y. Hua and A. Neville, Internal corrosion of carbon steel pipelines for dense-phase $CO_2$ transport in carbon capture and storage (CCS) – a review, *Int. Mater. Rev.*, 2017, **62**, 1–31.
67 S. Walspurger and H. A. J. Van Dijk, *EDGAR $CO_2$* purity. Type and quantities of impurities related to $CO_2$ point source and capture technology. A Literature study, 2012.
68 J. Wilcox, R. Haghpanah, E. C. Rupp, J. He and K. Lee, Advancing Adsorption and Membrane Separation Processes for the Gigaton Carbon Capture Challenge, *Annu. Rev. Chem. Biomol. Eng.*, 2014, **5**, 479–505.
69 Accenture, Industrial Clusters and the Path to Net Zero, **https://www.accenture.com/us-en/insights/utilities/industrial-clusters-net-zero-future**, 2021.
70 D. Kearns, H. Liu and C. Consoli, Technology readiness and costs of CCS, 2021.
71 C. Davis, *Oxy Looks to Ramp Permian Carbon Capture by Early 2024, Consider More JVs in Lower 48*, Natural Gas Intelligence, 2021.
72 B. Wrigh, Oxy To Sell Industry's First Net-Zero Oil, *J. Petrol. Technol.*, 2022, **https://www.oxy.com/news/news-releases/occidental-sk-trading-international-sign-first-agreement-for-net-zero-oil-created-from-captured-atmospheric-carbon-dioxide/**.
73 S. Van Paasen, *et al.*, *Int. J. Greenhouse Gas Control*, 2021, **109**, 103368.

74 BHI, Carbon Capture|Baker Hughes Carbon Capture, Baker Hughes, Inc., 2022.
75 Haru Oni, Tomorrow's fuel|Haru Oni, *e-Fuel*, 2021, **https://www.haruoni.com/#/en**.
76 D. S. Marlin, E. Sarron and Ó. Sigurbjörnsson, Process Advantages of Direct $CO_2$ to Methanol Synthesis, *Front. Chem.*, 2018, **6**, 446.
77 M. Bowker, Methanol Synthesis from $CO_2$ Hydrogenation, *ChemCatChem*, 2019, **11**, 4238–4246.
78 G. Zang, P. Sun, A. Elgowainy and M. Wang, Technoeconomic and Life Cycle Analysis of Synthetic Methanol Production from Hydrogen and Industrial Byproduct $CO_2$, *Environ. Sci. Technol.*, 2021, **55**, 5248–5257.
79 S. Stanbridge, *Teaching an old plant new tricks: The rise of the methanol plant revamp*, Hydrocarbon Processing, 2016.
80 S. Schemme, *et al.*, $H_2$-based synthetic fuels: A techno-economic comparison of alcohol, ether and hydrocarbon production, *Int. J. Hydrogen Energy*, 2020, **45**, 5395–5414.
81 F. Schorn, *et al.*, Methanol as a renewable energy carrier: An assessment of production and transportation costs for selected global locations, *Adv. Appl. Energy*, 2021, **3**, 100050.
82 E. Ruiz Martínez and J. M. Sánchez Hervás, Chemical Valorization of $CO_2$, in *Carbon Dioxide Utilization to Sustainable Energy and Fuels*, ed. Inamuddin, R. Boddula, M. I. Ahamed and A. Khan, Springer International Publishing, 2022, pp. 1–30, DOI: **10.1007/978-3-030-72877-9_1**.
83 S. M. Jarvis and S. Samsatli, Technologies and infrastructures underpinning future $CO_2$ value chains: A comprehensive review and comparative analysis, *Renewable Sustainable Energy Rev.*, 2018, **85**, 46–68.
84 R. Chauvy, N. Meunier, D. Thomas and G. De Weireld, Selecting emerging $CO_2$ utilization products for short- to mid-term deployment, *Appl. Energy*, 2019, **236**, 662–680.
85 S. Dang, *et al.*, A review of research progress on heterogeneous catalysts for methanol synthesis from carbon dioxide hydrogenation, *Catal. Today*, 2019, **330**, 61–75.
86 K. Stangeland, H. Li and Z. Yu, Thermodynamic Analysis of Chemical and Phase Equilibria in $CO_2$ Hydrogenation to Methanol, Dimethyl Ether, and Higher Alcohols, *Ind. Eng. Chem. Res.*, 2018, **57**, 4081–4094.
87 R. Dębek, F. Azzolina-Jury, A. Travert and F. Maugé, A review on plasma-catalytic methanation of carbon dioxide – Looking for an efficient catalyst, *Renewable Sustainable Energy Rev.*, 2019, **116**, 109427.
88 X. Jiang, X. Nie, X. Guo, C. Song and J. G. Chen, Recent Advances in Carbon Dioxide Hydrogenation to Methanol *via* Heterogeneous Catalysis, *Chem. Rev.*, 2020, **120**, 7984–8034.
89 FreSMe, *FReSMe Pilot Plant Operation*, 2021.
90 F. Geng, X. Zhan and J. C. Hicks, Promoting Methanol Synthesis and Inhibiting $CO_2$ Methanation with Bimetallic In–Ru Catalysts, *ACS Sustainable Chem. Eng.*, 2021, **9**, 11891–11902.
91 C. Zhou, *et al.*, Steering $CO_2$ hydrogenation toward C–C coupling to hydrocarbons using porous organic polymer/metal interfaces, *Proc. Natl. Acad. Sci. U. S. A.*, 2022, **119**, e2114768119.
92 **https://phys.org/news/2022-02-catalyst-carbon-dioxide-gasoline-efficiently.html**.
93 D. H. Kim, J. L. Park, E. J. Park, Y. D. Kim and S. Uhm, Dopant Effect of Barium Zirconate-Based Perovskite-Type Catalysts for the Intermediate-Temperature Reverse Water Gas Shift Reaction, *ACS Catal.*, 2014, **4**, 3117–3122.
94 Y. A. Daza and J. N. Kuhn, $CO_2$ conversion by reverse water gas shift catalysis: comparison of catalysts, mechanisms and their consequences for $CO_2$ conversion to liquid fuels, *RSC Adv.*, 2016, **6**, 49675–49691.
95 J. Kim, *et al.*, Methanol production from $CO_2$ using solar-thermal energy: process development and techno-economic analysis, *Energy Environ. Sci.*, 2011, **4**, 3122–3132.
96 J. Kim, T. A. Johnson, J. E. Miller, E. B. Stechel and C. T. Maravelias, Fuel production from $CO_2$ using solar-thermal energy: system level analysis, *Energy Environ. Sci.*, 2012, **5**, 8417–8429.
97 V. Dieterich, A. Buttler, A. Hanel, H. Spliethoff and S. Fendt, Power-to-liquid *via* synthesis of methanol, DME or Fischer–Tropsch-fuels: a review, *Energy Environ. Sci.*, 2020, **13**, 3207–3252.
98 P. Kallio, A. Pásztor, M. K. Akhtar and P. R. Jones, Renewable jet fuel, *Curr. Opin. Biotechnol.*, 2014, **26**, 50–55.
99 G. Zang, P. Sun, A. A. Elgowainy, A. Bafana and M. Wang, Performance and cost analysis of liquid fuel production from $H_2$ and $CO_2$ based on the Fischer-Tropsch process, *J. $CO_2$* Util., 2021, **46**, 101459.
100 A. P. Steynberg, M. E. Dry, B. H. Davis and B. B. Breman, Fischer–Tropsch Reactors, in *Studies in Surface Science and Catalysis*, ed. A. Steynberg, and M. Dry, Elsevier, 2004, ch. 2, vol. 152, pp. 64–195.
101 H. Er-rbib, C. Bouallou and F. Werkoff, Production of Synthetic Gasoline and Diesel Fuel from Dry Reforming of Methane, *Energy Procedia*, 2012, **29**, 156–165.
102 B. Yao, *et al.*, Transforming carbon dioxide into jet fuel using an organic combustion-synthesized Fe-Mn-K catalyst, *Nat. Commun.*, 2020, **11**, 6395.
103 B. Stefansson, *Power and $CO_2$ emissions to methanol|CRI*, 2015.
104 CORDIS, MefCO2 (Synthesis of methanol from captured carbon dioxide using surplus electricity), 2020, **https://cordis.europa.eu/project/id/637016/reporting/it**.
105 IRENA, Innovation Outlook: Renewable Methanol, 2021, **https://www.irena.org/publications/2021/Jan/Innovation-Outlook-Renewable-Methanol**.
106 TotalEnergies, TotalEnergies, Sunfire and Fraunhofer give the go-ahead for green methanol in Leuna, *TotalEnergies*, 2021.
107 G. Leonzio, State-Of-The-Art Overview of CO2 Conversions, in *Carbon Dioxide Utilization to Sustainable Energy and Fuels*, ed. Inamuddin, R. Boddula, M. I. Ahamed and A. Khan, Springer International Publishing, 2022, pp. 335–353, DOI: **10.1007/978-3-030-72877-9_18**.
108 A. Benzinger, *Construction begins on world's first integrated commercial plant*, Siemens Energy, 2021.
109 HIF Global, Haru Oni Demonstration Plant, *HIF Global*, 2022.
110 Methanol Institute, Renewable and Biomethanol Projects 2021|Methanol Institute, Methanol Institute, 2022.

111 J. Lane, *ENVIA suspends operations, Velocys renews focus on Mississippi, UK projects*, Biofuels Digest, 2018, **https://www.biofuelsdigest.com/bdigest/2018/09/11/envia-suspends-operations-velocys-renews-focus-on-mississippi-uk-projects/**.
112 Velocys, Velocys: Oklahoma City plant on track to reach final capacity, *Velocys*, 2017.
113 N. Hargreaves, *Roll out of smaller scale GTL technology at ENVIA Energy's plant in Oklahoma City, USA|Velocys*, 2017.
114 Siemens, The global energy transition will be based on the hydrogen economy, Siemens Energy, 2021.
115 Siemens, *Power-to-Kerosene|Green hydrogen for climate-neutral aviation*, 2021, **https://assets.siemens-energy.com/siemens/assets/api/uuid:34bec577-f25a-48cd-8618-6dd848b38515/FactsheetWerlteEN.pdf**.
116 Velocys, Velocys launches Bayou Fuels|Velocys, *Velocys*, 2021.
117 J. Brinkman and A. Schilderman, Synkero builds facility in the port of Amsterdam, producing sustainable aviation fuel from $CO_2$, *SkyNRG*, 2021.
118 Synkero, Synkero: Futureproof Aviation, *Synkero*, 2021.
119 R. van Roon, Zenid®|Jet fuel from air, *Zenid®*, 2021, **https://zenidfuel.com/**.
120 INFINIUM, Infinium™ Enters into Strategic Alliance with Denbury for Ultra-Low Carbon Fuels Projects in Texas, Continuing Development Momentum, *Infinium*, 2022.
121 Biofuels International, ExxonMobil to supply SAF as part of Singapore pilot|Biofuels International Magazine, *Biofuels International*, 2022.
122 E. Moses, *Oxy Low Carbon Ventures Selects Worley for Services Contract on Canadian Direct Air Capture (DAC)-to-Fuels Facility*, Oxy Low Carbon Ventures 2021.
123 Norsk e-Fuel, COMING SOON: GREEN JET-FUEL FROM MOSJØEN, NORWAY, *Norsk e-Fuel*, 2022.